4 Dynamics of SIV infection of follicular T cells

4.1 Introduction and aims

HIV/SIV infects primate cells using CD4 alongside CCR5 and CXCR4 as co-receptors[16,20,21]. However, not all CD4 T cells are equally infected: it is now well established that HIV preferentially infects memory T cells[363] and HIV-specific CD4+ T cells. Efforts to further define the features of infected cells have focused on chemokine, activation, and localization markers in search of signatures of preferentially infected T cell subsets. Resting memory CD4 T cells are highly infected[364], with memory CD57- CD4+ T cells containing more HIV gag DNA than terminally differentiated CD57+ T cells. CCR6+RORγt+ Th17 cells were shown to be preferentially infected in very acute SIV infection of macaques in vaginal transmission of macaques[365], and CCR6+CCR4+ and CCR6+CXCR3+ CD4 T cells were found to be highly permissive to HIV-1 infection [366].

Recently follicular helper T cells (TFH), located in secondary lymphoid organs, are cited as a major compartment of HIV/SIV infection in CD4+ T cells[170,172,174]. Preferential infection of TFH, which are critical to antibody development and maturation, presents an additional impairment to the immune response to HIV/SIV. TFH provide B cell help in germinal centers to promote somatic hypermutation and class switch recombination, key components of the development of an effective humoral immune response. In a study by Yamamoto et al [367], the quality and quantity of TFH were closely related to the induction of broadly neutralizing antibody responses in a SHIV model of infection. Work by Cubas et al[173]. showed that TFH in chronic HIV infection are unable to provide adequate B cell help. Finally, recent work has shown that the B cell follicle may represent a sanctuary of productive infection in elite controller macaques that is protected from effective CTL, with on-going viral replication in TFH located in the follicle and germinal centers[174]. Questions remain about the timing of infection of TFH and how big of a role they play in supporting HIV/SIV replication throughout infection. Here, we aim to measure the contributions of follicular T cells and other CD4+ T cell subsets to the overall pool of virus and infected cells, from initial infection through peak viremia to viral setpoint. We profile changes in activation and chemokine markers on CD4+ T cells throughout early infection and measure SIV DNA and RNA in memory T cell subsets to determine the phenotype and characteristics of productively and persistently infected CD4 T cells in SIV infection.

The aims of this chapter are to:

- Profile changes phenotypic changes in chronically infected HIV PBMC and acutely and chronically SIV-infected PBMC and lymph nodes
- Design primers, probes, and standards to quantify spliced SIV RNA
- Investigate CD4 downregulation as a phenotypic marker of active SIV infection
- Identify productively infected CD4 T cells using qPCR and SIV RNA probes in conjunction with flow cytometry phenotyping panels

4.2 Results

4.2.1 Chemokine and activation markers on CD4 T cell subsets throughout HIV/SIV infection

HIV/SIV infection induces massive changes in the inflammation and activation of T cells in lymph nodes, including alterations in T cell trafficking; changes in architecture of lymph nodes, bone marrow, and thymus; and shifts in the relative proportions of naïve and memory T cells [23]. We first wanted to examine, using flow cytometry profiling of surface markers, changes in the activation and chemokine markers on subsets of CD4 T cells in acute and chronic infection. Flow cytometry panels were designed and tested to ensure distinct separation of markers for longevity (CD127/ILR-a), activation (ICOS, CD25, PD-1), and trafficking (CCR6, CCR4, CXCR3). CD127 plays an important role in T cell development and antigen-specific responses, and is down-regulated upon expansion[368,369]. ICOS is expressed on activated T cells and enhances proliferation, cytokine secretion, and secretion of antibodies by B cells[370]. PD-1 is a negative regulator of T cells and plays an important role in infectious immunity, tumor immunity, and autoimmunity[371]. CD25 is part of the IL-2 receptor and marks a variety of activated cells[372]. CCR6 is the receptor for MIP3-α, is expressed on Th17 cells, and plays a role in their migration into inflamed tissues[373]. CCR4 is associated with Th2 cells while CXCR3 is associated with Th1 cells and both play a role in trafficking activated cells to sites of inflammation[374,375].

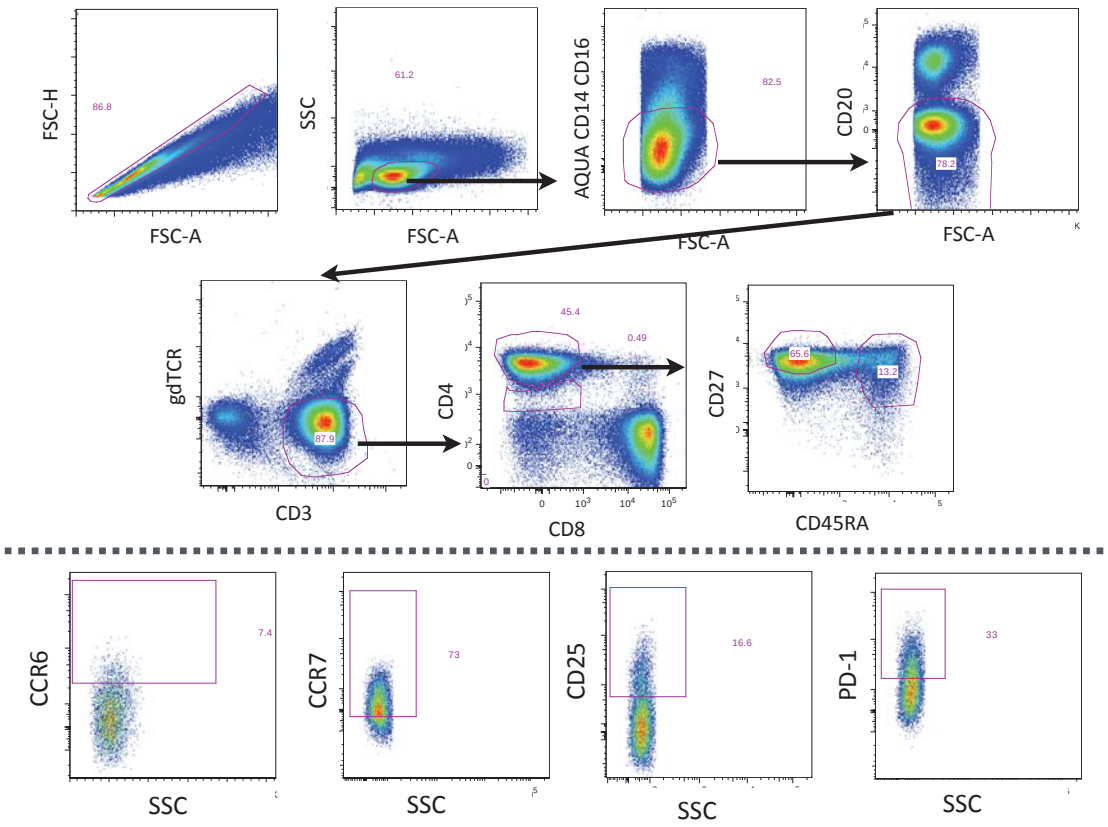

Fig. 4.1 Representative gating schematic for phenotyping of HIV-infected PBMC. PBMC were stained and acquired on a flow cytometer, gating on forward/side scatter, lymphocytes, live CD14-CD16-CD20-gdTCR-CD3+ T cells, and subsequently on CD8- CD4 bright and CD8- CD4 dim expression. Expression of CCR6, CCR7, CD25, and PD-1 was measured on CD45RA- CD27+ memory T cells.

4.2.1.1 Expression patterns in HIV-positive PBMC

In an initial assessment of T cell phenotype in infection, we profiled five PBMC samples from chronically HIV-infected, virally suppressed donors on combination antiretroviral therapy and compared them to five uninfected controls. CD4 is down-regulated during active infection[52], and by examining CD4 dim cells (that are CD3+ CD8-) separately from CD4 bright cells we hypothesized that we might distinguish features of infected cells by examining an enriched population (Fig 4.1). There were fewer CCR6+ CD4 bright T cells in HIV infection than in uninfected controls (means of 6.1% in HIV positive samples and 17.1% in uninfected controls), but no difference in expression on CD4 dim cells (Fig 4.2). CCR7 expression was unchanged between CD4 high and dim cells in HIV positive samples but in HIV negative samples, was lower on CD4 high cells (43.2%) than on CD4 dim cells (66.1%). Though it did not reach statistical significance, we observed lower expression of CD25 in both populations in HIV infected samples than in uninfected samples (means of 13.7% and 14.3% compared to 19.4% and 23.0%). This is in agreement with published work showing depletion of CD25+ T cell subsets in HIV infection [376]. PD-1 expression was significantly higher in CD4 high HIV positive samples (34.4%) than CD4 dim uninfected samples

(11.9%), and higher than CD4 high uninfected (17.9%) and HIV infected CD4 dim (20.0%). Overall, HIV positive samples were characterized by higher expression of CCR7 and PD1 and lower expression of CCR6.

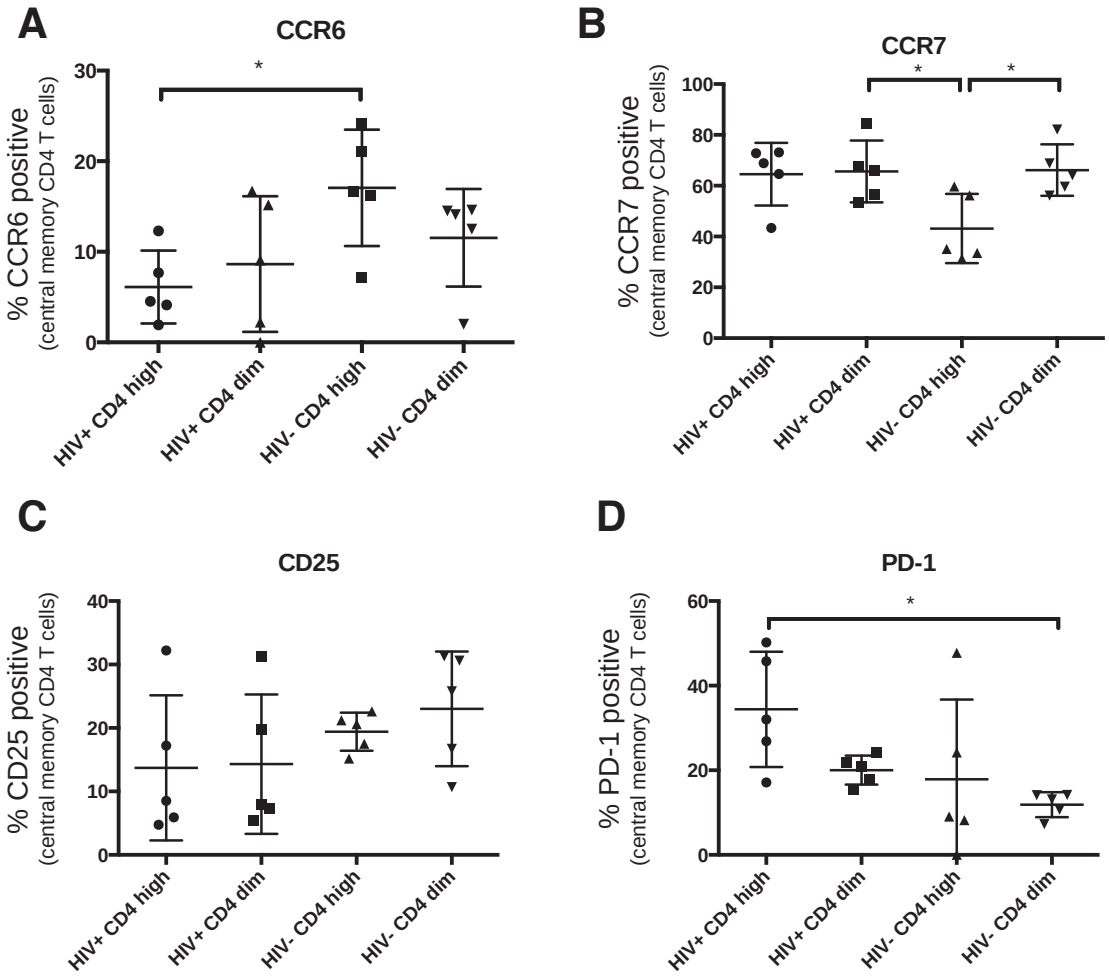

Fig 4.2 Expression patterns of cell surface receptors in HIV positive and negative PBMC. Percentage of central memory CD4 T cells expressing (A) CCR6, (B) CCR7, (C) CD25, and (D) PD-1 on CD4 high and dim populations in PBMC from HIV infected and uninfected donors. Significant differences were determined using a one way ANOVA test.

4.2.1.2 Expression patterns on uninfected, acutely SIV-infected, and chronically SIV-infected lymph node samples

To further investigate changes in T cell phenotypes during SIV infection, we stained and analysed lymph nodes from rhesus macaques infected with SIVmac251, with biopsies taken at the acute stage (5-14 days), chronic stage (6 months to 2 years), or uninfected controls. We looked at expression of chemokine and activation markers on CD4 T cells and CD3+ CD4 dim cells (to capture actively infected cells), and within the central memory compartment at three populations: TFH (defined here as PD1++CXCR5++ cells), CXCR5+ cells, and CXCR5- cells (gating strategy detailed in Fig 4.3). CXCR5 and PD-1 together identify CD4+ T cells located in B cell follicles, but without additional markers it is impossible to segregate follicular helper T cells (TFH) from follicular regulatory T cells (TFR), which do not directly

provide B cell help. In this work, the term “TFH” is used to refer to both CXCR5+PD1+ and CXCR5++PD1++ CD4+ T cells and is inclusive of TFR.

First, we looked at expression of CCR4 was lower on CD4 T cells from chronically infected macaques than uninfected controls (mean of 24% vs. 48%), with acute samples slightly higher than chronic samples with mean expression of 36% (Fig 4.4A). Uninfected samples had higher expression of CCR6 (21%) than acutely infected (10%) or chronically infected (10%) samples (Fig 4.4B). CXCR3 expression was lower on acutely infected samples (28%) than on chronically infected samples (44%) (Fig 4.4C). SLAM expression was higher in chronic samples than uninfected controls (32% vs. 21%) and acute samples had a wide range of SLAM expression (from 10% to 35%) (Fig 4.4D). There was no significant difference in expression of CD25 between samples, but acutely infected samples had significantly higher expression of CD127 (85%) than chronically infected samples (55%) or uninfected samples (66%) (Fig 4.4 E-F) Finally, ICOS expression was lower on acute samples (26%) than chronic samples (54%) (Fig 4.4G). In CD4 dim cells, there was no difference in expression of CCR6, CXCR3, or SLAM between acute, chronic, or uninfected samples (Fig 4.5B-D). CCR4 expression and CD127 expression were significantly lower in chronic infection on CD4 dim cells than in acute or uninfected samples (Fig 4.5 A and F), but ICOS expression was significantly higher in chronically infected samples (Fig 4.5 G). ICOS, CCR4, and CD127 expression on CD4 dim cells mirrored expression patterns in CD4 high cells, but expression of CD127 was lower overall in CD4 dim cells. Overall, lymph node CD4 T cells in acute infection had higher CCR4, CD127, and ICOS expression and lower CXCR3 expression than chronic infection. Chronically infected lymph node samples had lower CCR4, CCR6, and CD127 than uninfected samples.

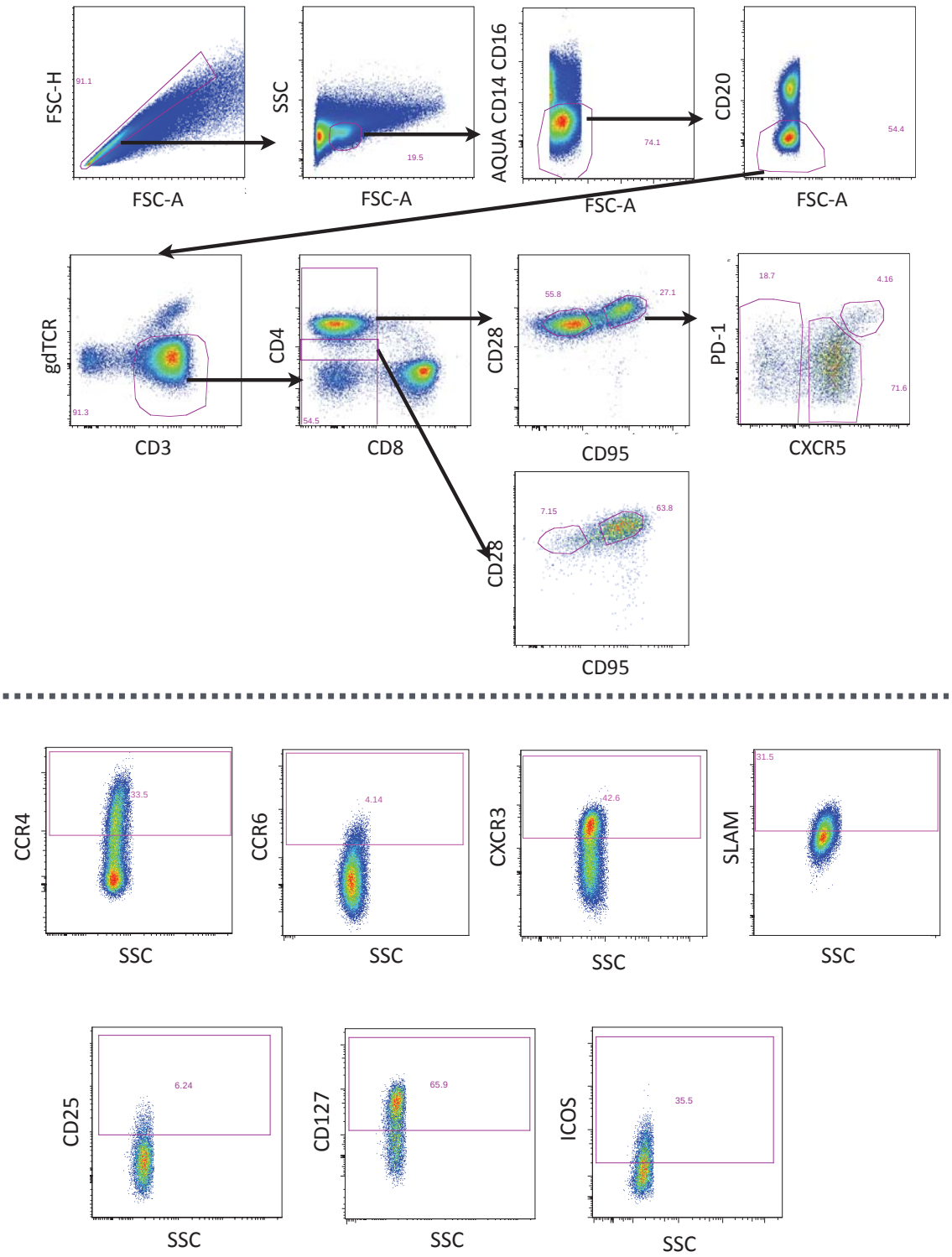

Fig 4.3 Representative gating schematic for phenotyping of SIV-infected and uninfected lymph node biopsies. Lymph node single cell suspensions were stained and acquired on a flow cytometer, gating on forward/side scatter, lymphocytes, live CD14-CD16-CD20-gdTCR- CD3+ T cells, and subsequently on CD8- CD4 bright and CD8- CD4 dim expression. Expression of CCR4, CCR6, CXCR3, SLAM, CD25, CD127, and ICOS was measured on CD28+CD95+ memory T cells.

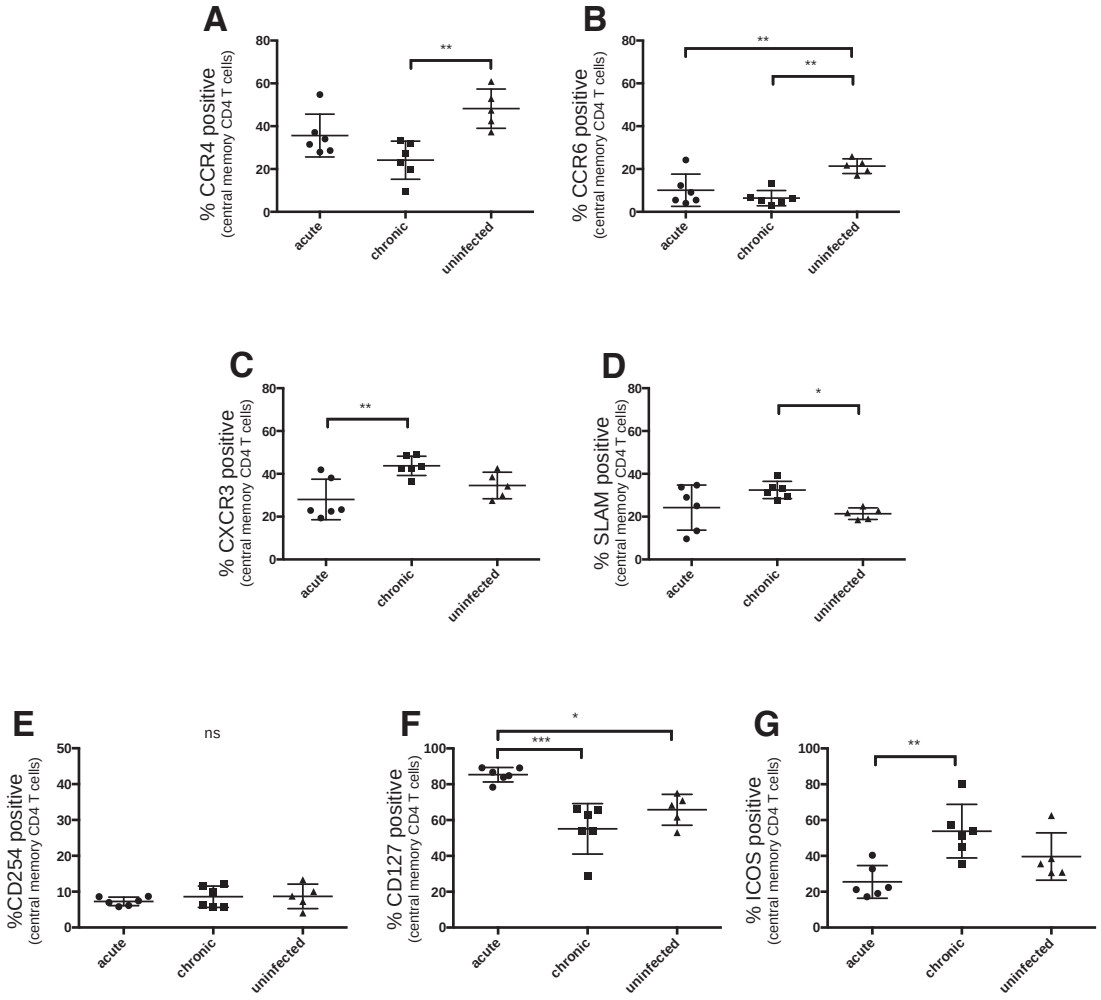

Fig 4.4 Expression patterns of cell surface receptors on lymph node memory CD4 high T cells in SIV infection. Percentage of central memory CD4 high T cells expressing (A) CCR4, (B) CCR6, (C) CXCR3, (D) SLAM, (E) CD25, (F) CD127, and (G) ICOS in acutely infected, chronically infected, and uninfected lymph nodes. Significant differences were determined using a one way ANOVA test.

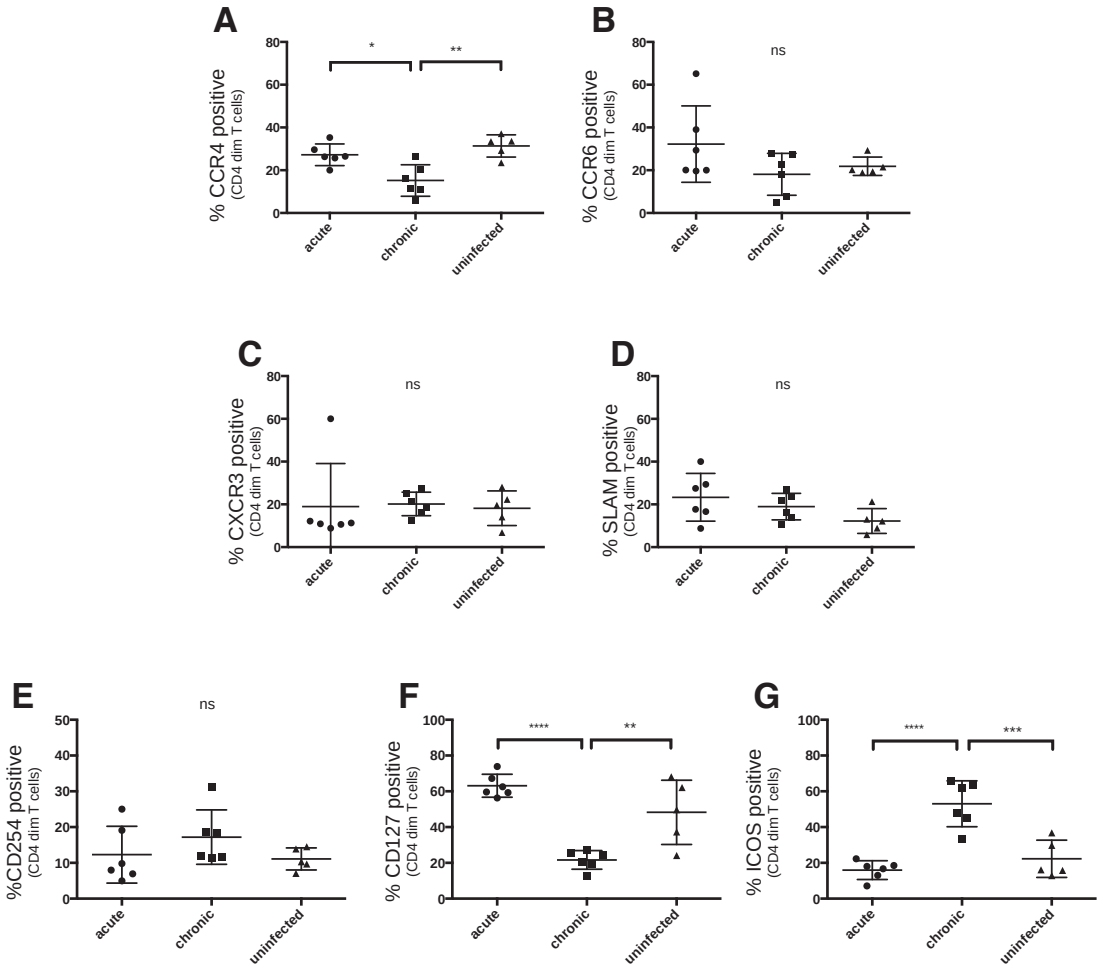

Fig 4.5 Expression patterns of cell surface receptors on lymph node CD4 dim T cells in SIV infection. Percentage of central memory CD4 dim T cells expressing (A) CCR4, (B) CCR6, (C) CXCR3, (D) SLAM, (E) CD25, (F) CD127, and (G) ICOS in acutely infected, chronically infected, and uninfected lymph nodes. Significant differences were determined using a one way ANOVA test.

Central memory T cells are not homogenous but rather represent a diverse population of cells with different activation and localization histories. As CD4 T cells migrate from the T cell zone into the B cell follicle and into germinal centers, they down-regulate CCR7 and up-regulate CXCR5. We divided CD95+CD28+ central memory CD4+ T cells into three populations based on expression of PD-1 and CXCR5 to distinguish between cells located in the T cell zone (CXCR5-), B cell follicle (CXCR5+PD1+) and within germinal centers (CXCR5++PD1++), and measured expression of several chemokine and activation markers within each population. The term TFH is used to refer to CXCR5+PD1+ and CXCR5++PD1++ cells and is inclusive of TFR, which are not distinguished from TFH in this panel

In CXCR5- cells, expression of CCR4, CCR6, CXCR3, SLAM, ICOS, and CD127 followed the same patterns as in overall central memory cells (Fig 4.6). CCR4 expression was higher in

acute CXCR5- samples than in overall central memory (49% vs. 35%, Fig 4.6A) and SLAM expression was higher in chronic CXCR5- samples than in overall central memory (55% vs. 32%, Fig 4.6D). However, CD25 expression was significantly lower on acute samples (mean of 6.7%) than on chronic samples (13.8%) or uninfected samples (13.1%) (Fig 4.6 E). In CXCR5+ cells, patterns of CCR6, CXCR3, CD127, and ICOS expression were unchanged from central memory cells (Fig. 4.7), but CCR4 expression was lower in acute, chronic, and uninfected than in the corresponding samples in central memory. CCR4 expression in TFH was lower than central memory or CXCR5+ cells, with a mean of 7.5% in acute samples and 4.2% in chronic samples. CCR6 expression was lowest in CXCR5+ cells in acute and chronic infection, and SLAM expression was highest in CXCR5+ chronically infected cells. However, there was no difference in SLAM staining on TFH between acute, chronic, and uninfected samples. ICOS expression was highest on TFH in all samples, but in chronic infection most TFH (92%) expressed ICOS compared to 47% of CXCR5+ and 46% of CXCR5- cells. TFH also had lower expression of CD127 in all samples, but acute samples still maintained higher expression of CD127 than in chronic or uninfected samples. Thus, TFH exhibit distinct patterns of expression of chemokine and activation markers in acute and chronic infection from central memory T cells and from CXCR5+ and CXCR5- memory subsets.

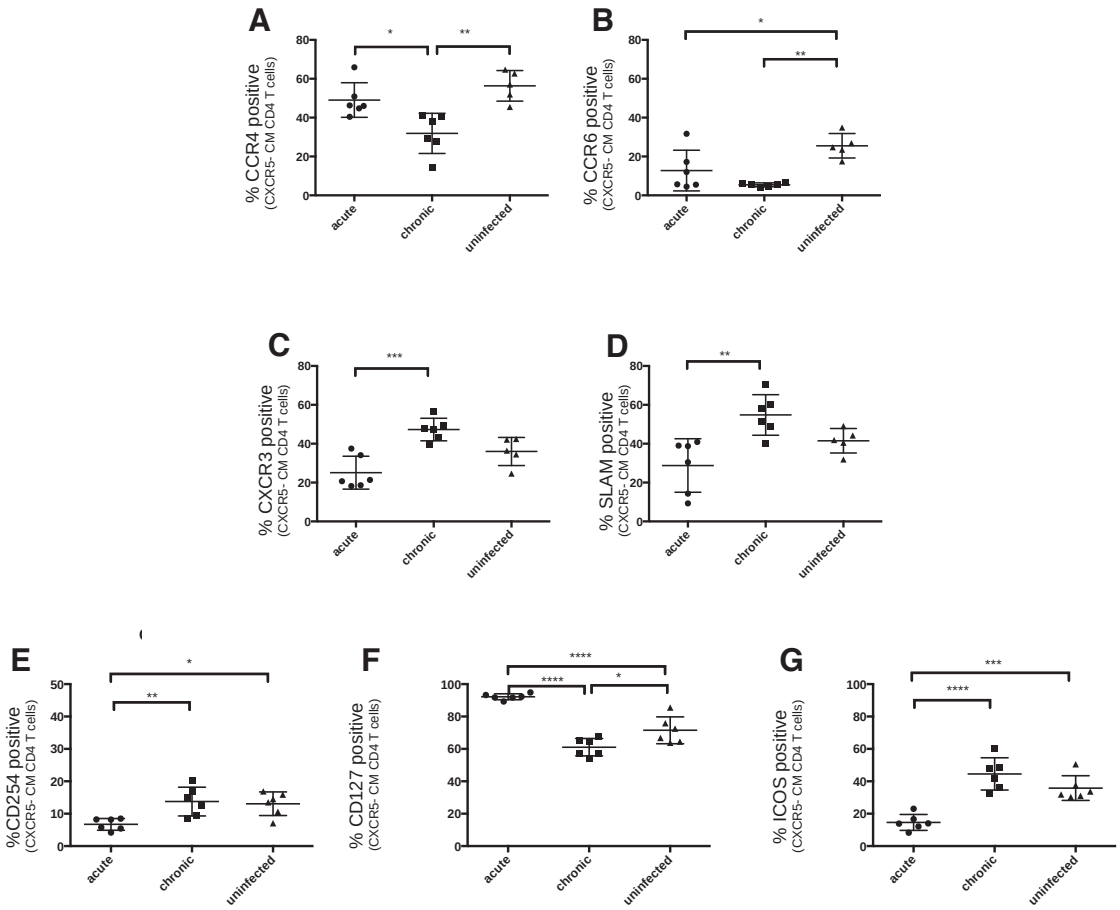

Fig 4.6 Expression patterns of cell surface receptors on lymph node CXCR5- memory CD4 T cells in SIV infection. Percentage of CXCR5- central memory CD4 T cells expressing (A) CCR4, (B) CCR6, (C) CXCR3, (D) SLAM, (E) CD25, (F) CD127, and (G) ICOS in acutely infected, chronically infected, and uninfected lymph nodes. Significant differences were determined using a one way ANOVA test.

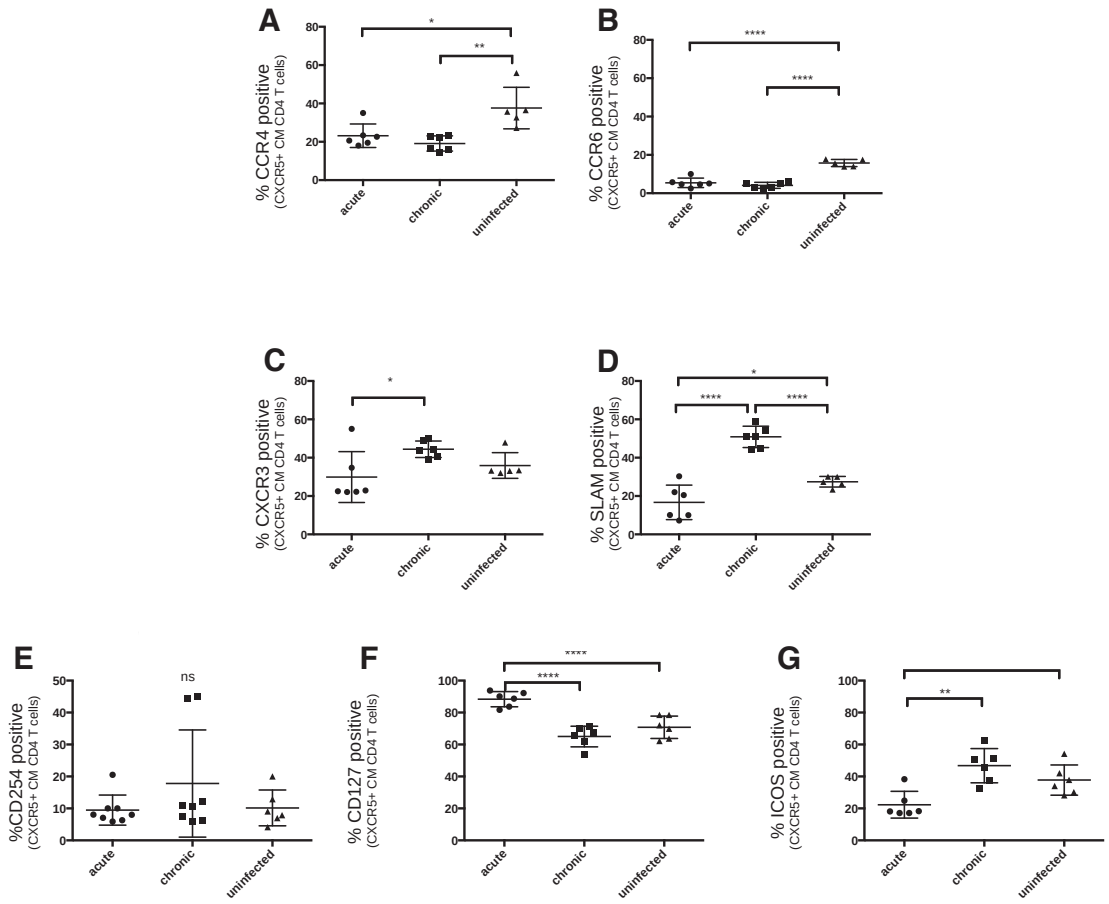

Fig 4.7 Expression patterns of cell surface receptors on lymph node CXCR5+ memory CD4 T cells in SIV infection. Percentage of CXCR5+ central memory CD4 T cells expressing (A) CCR4, (B) CCR6, (C) CXCR3, (D) SLAM, (E) CD25, (F) CD127, and (G) ICOS in acutely infected, chronically infected, and uninfected lymph nodes. Significant differences were determined using a one way ANOVA test.

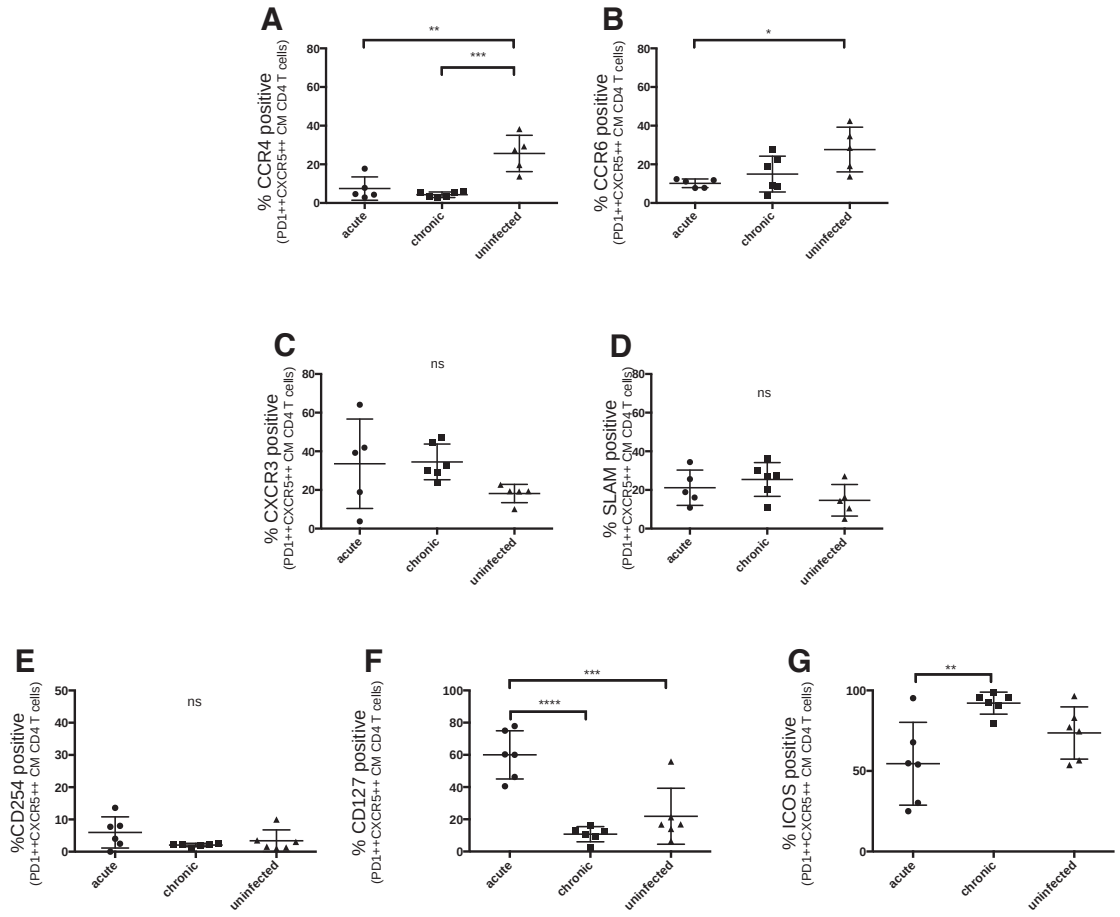

Fig 4.8 Expression patterns of cell surface receptors on lymph node TFH CD4 T cells in SIV infection. Percentage of T follicular helper (CXCR5++PD1++) CD4 T cells expressing (A) CCR4, (B) CCR6, (C) CXCR3, (D) SLAM, (E) CD25, (F) CD127, and (G) ICOS in acutely infected, chronically infected, and uninfected lymph nodes. Significant differences were determined using a one way ANOVA test.

4.2.2 Development of spliced RNA primers and probes

4.2.2.1 Design of primers probes & testing

HIV/SIV infection at the cellular level can be measured in several ways, depending on the type of sample and the research questions. In viral outgrowth assays, resting CD4 T cells from infected donors are activated and cultured alongside uninfected cells, and virus in cell supernatants is measured (typically via ELISA) after days to weeks of cell culture. Donor cells can be cultured in limiting dilution to estimate the frequency of infected cells. HIV/SIV constructs containing green fluorescent protein (GFP) can be used in cell culture infections to measure productive infection via flow cytometry. Quantitative PCR and reverse transcription PCR detect the presence of nucleic acids, and in the case of a retrovirus, can indicate whether transcription has occurred based on the presence of viral RNAs. We used PCR and reverse transcription PCR to quantify the presence of viral nucleic acids in T cell subsets, to understand whether infection was productive (i.e. not only had virus integrated into the cellar genome but that the virus was able to replicate and differentiate between early spliced RNAs and late unspliced RNA). Well-defined primers and probes to detect SIVmac251 Gag DNA

and RNA have been previously published by Lifson et al[326], and we generated absolute standards for that primer/probe set alongside the spliced RNA standards. To measure spliced RNA, we designed primers and probes that spanned the D4/A7 splice site in the SIVmac251 genome (Fig 4.9). To ensure maximum sensitivity to sequence heterogeneity within samples, we used a consensus alignment of 15 SIV full genome sequences including mac251, mac239 and smE660 to design 21-30 nucleotide primers and 21-33 nucleotide probes, and included degenerate bases. The probes span the splice site such that full-length RNAs and singly spliced RNAs (env, vif, tat) do not contain the target sequence. We verified the specificity of the primers by doing side-by-side qPCR with SIV DNA (containing only full length genomes) and qRT-PCR with SIV RNA (containing a mix of full length and spliced genomes), both extracted from in vitro infections of H9 cells with SIVmac251 (Fig 4.10). We verified infection in both cell lines and in primary cells using p24 staining, with 8% of H9 cells infected at 5 days post infection and saw no staining in the uninfected controls. The culture was split and DNA and RNA were extracted for qPCR, qRT-PCR, and synthesis of standards. After testing several combinations of primers and probes, we selected three forward primers, three reverse primers, and 3 probes that had the maximum sensitivity The tat/rev primers and probes did not produce any signal in the DNA qPCR, but detected spliced RNA in the qRT-PCR (Figure 4.11).

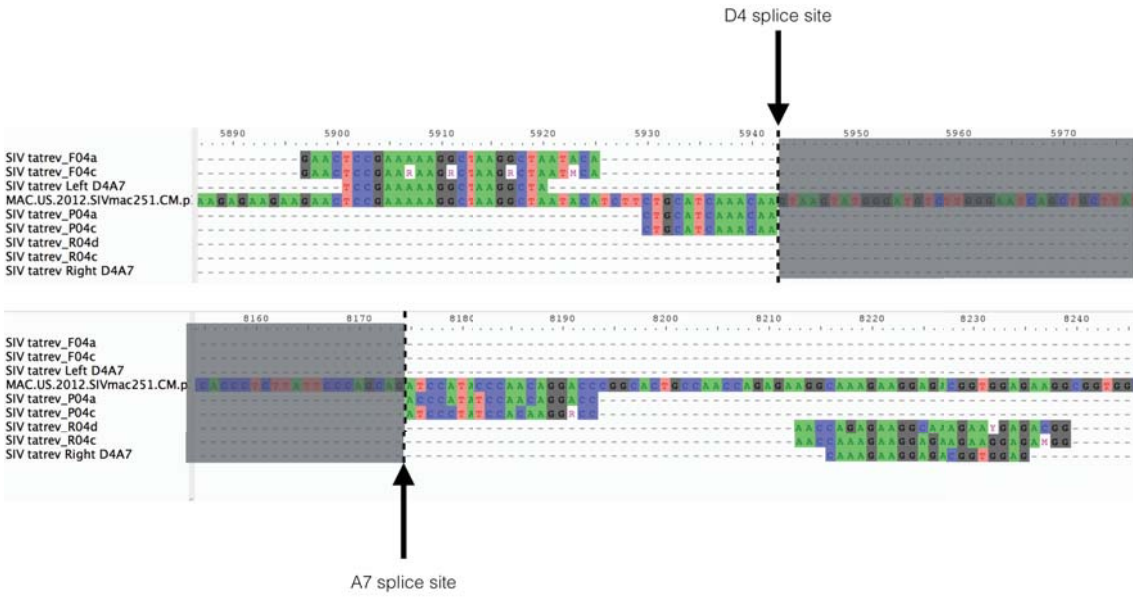

Fig 4.9 Primers and probes for spliced tat/rev RNA detection. Six primers (three forward, three reverse) and two probes were designed to uniquely amplify spliced SIV RNAs. Probes spanned the D4/A7 splice site, and all sequences were designed using a consensus alignment of SIV genomes.

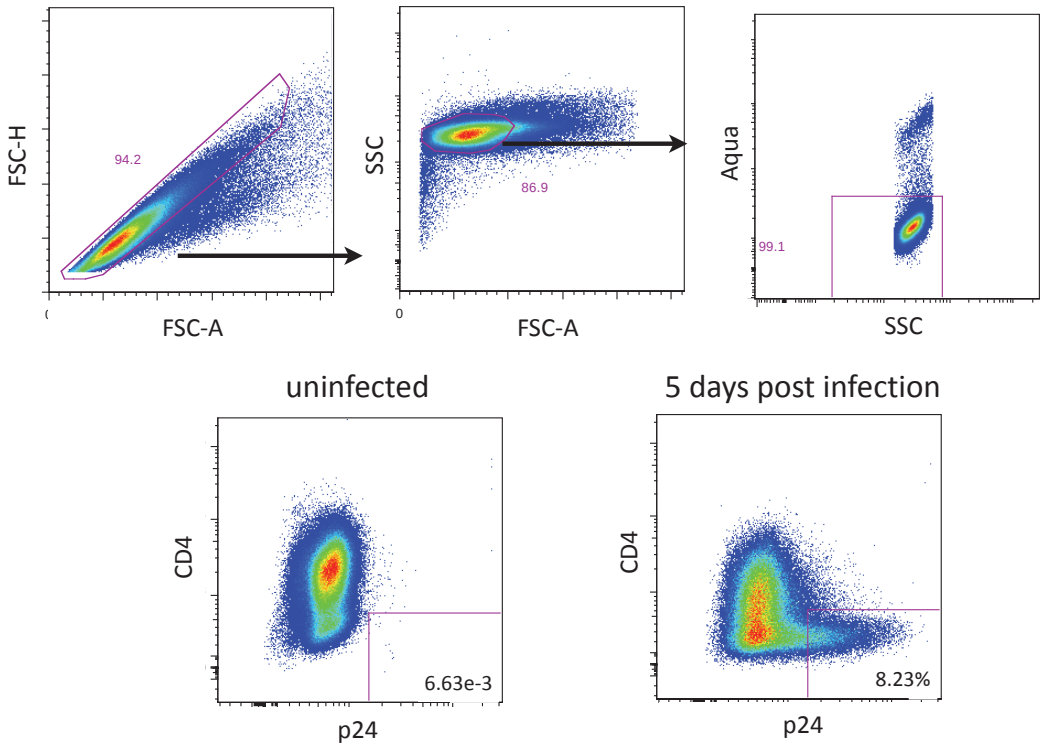

Fig. 4.10 *in vitro* infection of H9 cells. Cell line H9 was cultured and infected with SIVmac251 for 5 days to generate stocks of viral RNA and DNA for creation of SIV standards. Productive infection was verified using p24 staining on CD4 down-regulated cells.

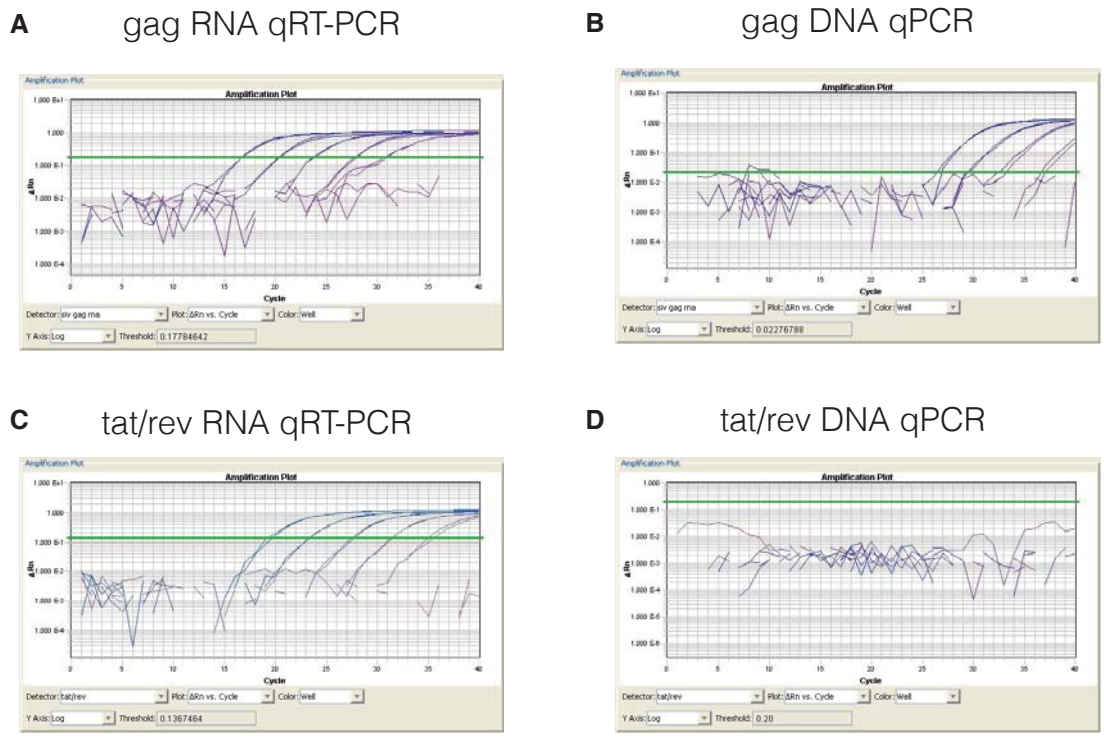

Fig 4.11 Tat/rev primers and probes uniquely amplify RNA. Serial dilutions of RNA (A, C) and DNA (B, D) from SIV-infected cells were used with gag (A, B) and tat/rev (C, D) primers and probes to verify linear amplification of the target RNA or DNA.

4.2.2.2 Synthesis of standards for absolute quantification of spliced and unspliced RNA

To quantify spliced SIV RNA, we used the tat/rev primers to amplify a 106 nucleotide region spanning the D4/A7 splice site and used the pGEM-T vector to transform DH5-a cells to produce plasmids containing the target sequence. Twenty recombinant colonies were picked and the presence of the DNA fragment was confirmed via qPCR. Samples were sent for Sanger sequencing to confirm that the correct, un-mutated sequence was present in the plasmids before purification for RNA synthesis using MEGAscript T7 Transcription enzymes. After RNA synthesis and purification, samples were re-checked for detection of SIV RNA using qPCR and qRT-PCR, and RNA was quantified (Fig 4.12) and diluted to yield standards ranging from 100 copies to $1x10^7$ copies. We performed the same protocol using published SIV gag primers to generate gag RNA standards.

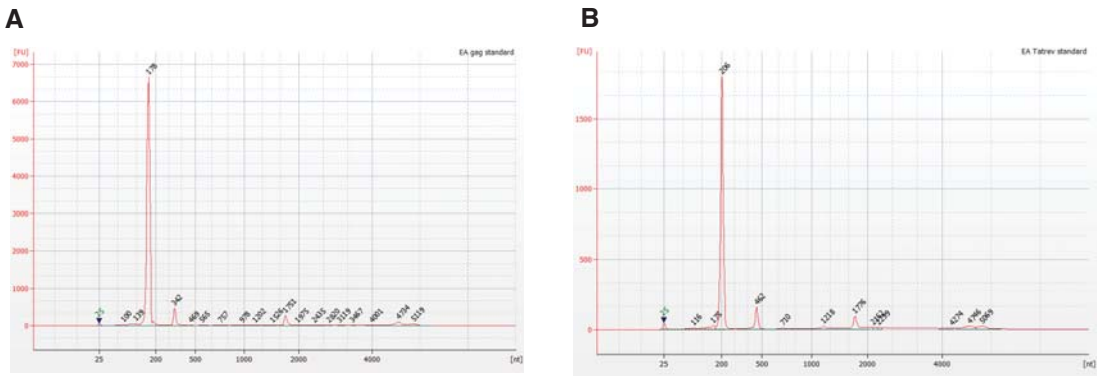

Fig 4.12 High sensitivity quantification of RNA standards for gag and tat/rev primers and probes. (A) SIV gag and (B) SIV tat/rev RNA standards were verified for size and quantity for serial dilution of standards for qRT-PCR. Bioanalyzer traces showed purity of product (>99%) of the appropriate length.

4.2.3 CD4 down-regulation as a marker of active infection

4.2.3.1 Sorting and quantification of SIV in CD4 dim cells

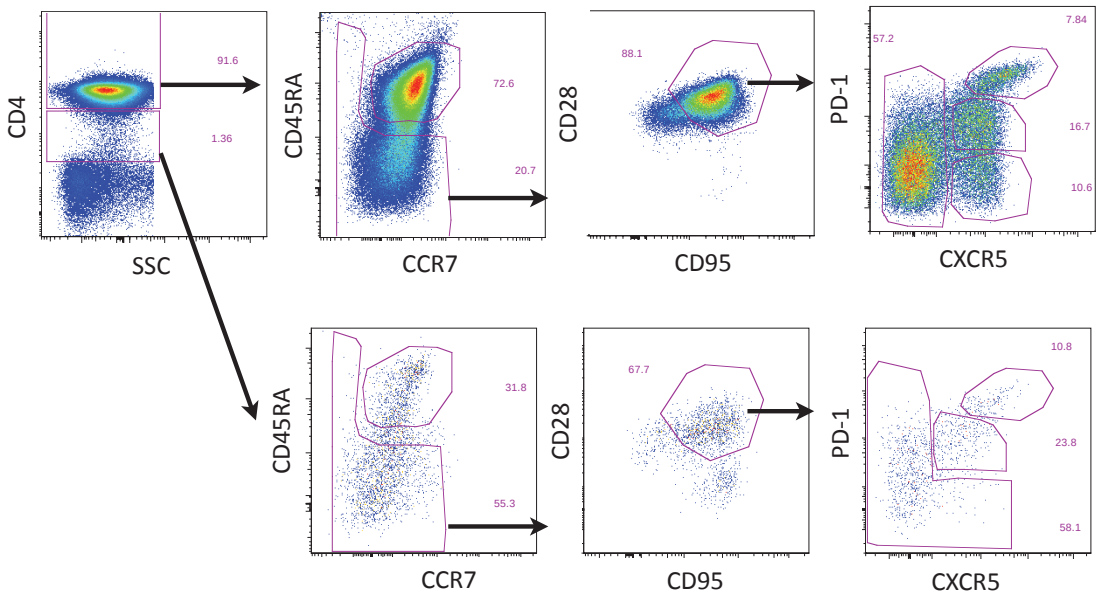

Fig 4.13 Representative gating schematic for sorting CD4 T cells subsets from acutely SIV-infected lymph node biopsies. Lymph node single cell suspensions were stained and sorted after gating on forward/side scatter, lymphocytes, live CD14-CD16-CD20-gdTCR-CD8- CD3+ T cells (as in Fig. 4.3) and subsequently on CD4 bright and CD4 dim expression. Four populations, based on expression of CXCR5 and PD-1, were sorted from memory (CD45RA-CD28-CD95+) CD4 high cells, while three were sorted from CD4 dim cells. Naïve cells (CD45RA+CCR7+CD28+CD95-) cells were sorted from CD4 high cells.

SIV protein nef is produced early in viral replication and down-regulates several surface markers including CD3, CD4, and MHC I. To confirm that CD4 dim CD3+ cells contain a high proportion of actively infected cells, we sorted naïve cells and memory T cells from CD4 high and dim populations, and quantified both spliced and unspliced SIV RNA from acutely infected (5-28 days post infection) lymph node biopsies. The gating scheme is similar to previous samples but with the addition of CD45RA and CCR7 to define central memory populations (Fig. 4.13). Due to the low numbers of CD4 dim cells, we sorted only three subsets from central memory to compare TFH (both PD1++CXCR5++ and PD1+CXCR5+) to non-TFH. Copy numbers of Gag RNA per cell were similar between all four CD4 high memory populations (median of 0.065 to 0.16), and were significantly higher in CXCR5++PD1++, CXCR5+PD1+, and CXCR5- cell than in naïve CD4 T cells (Fig 4.14). Copy numbers were slightly higher in PD1++CXCR5++ cells than the other populations (0.16 copies/cell vs. 0.078, 0.091, and 0.065 copies/cell). There were higher copy numbers of spliced tat/rev RNA in PD1++CXCR5++ (1.3 copies/cell) and PD1+CXCR5+ (1.7 copies/cell) cells than in non TFH (0.096 in CXCR5+ and 0.33 in CXCR5-), and virtually no spliced tat/rev RNA detected in naïve cells. Within CD4 dim cells, there was no difference between the copy numbers per cell of spliced or unspliced SIV RNA in CXCR5++PD1++, CXCR5+PD1+, and non TFH (gag RNA 0.25 copies- 0.72 copies, tat rev 1.1 copies-2.6

copies/cell) (Fig. 4.15). However, in comparing the copy numbers between high and dim cells, there were significantly higher copy numbers of both gag RNA and tat/rev RNA in CD4 dim CXCR5++PD1++ cells, and significantly higher copy number of gag RNA in CXCR5+PD1+ cells (Fig 4.16). While there was considerable sample-to-sample variability between the copies of gag and tat/rev RNA per cell, copy numbers were consistently higher in CD4 dim cells than in CD4 high cells. Thus, CD4 dim cells likely have more productively infected, i.e. producing high copy numbers of spliced and unspliced RNA during active infection, cells than any subset of CD4 bright cells.

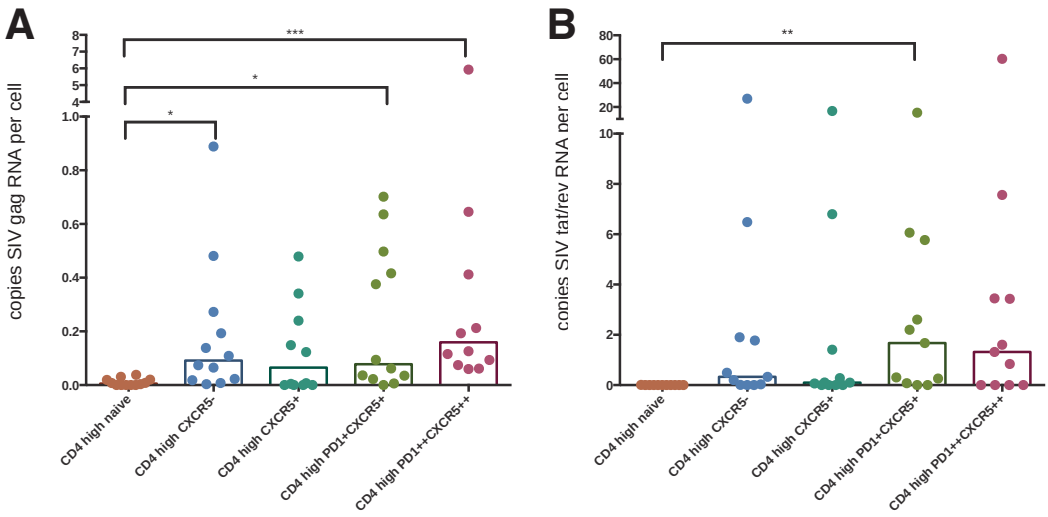

Fig 4.14 SIV RNA copies in CD4 bright T cell subsets. (A) unspliced gag RNA and (B) spliced tat/rev RNA copies per cell in naïve and CXCR5-, CXCR5+, PD1+CXCR5+, and PD1++CXCR5++ CD4 bright memory T cells. Significant differences were determined using the one-way ANOVA test.

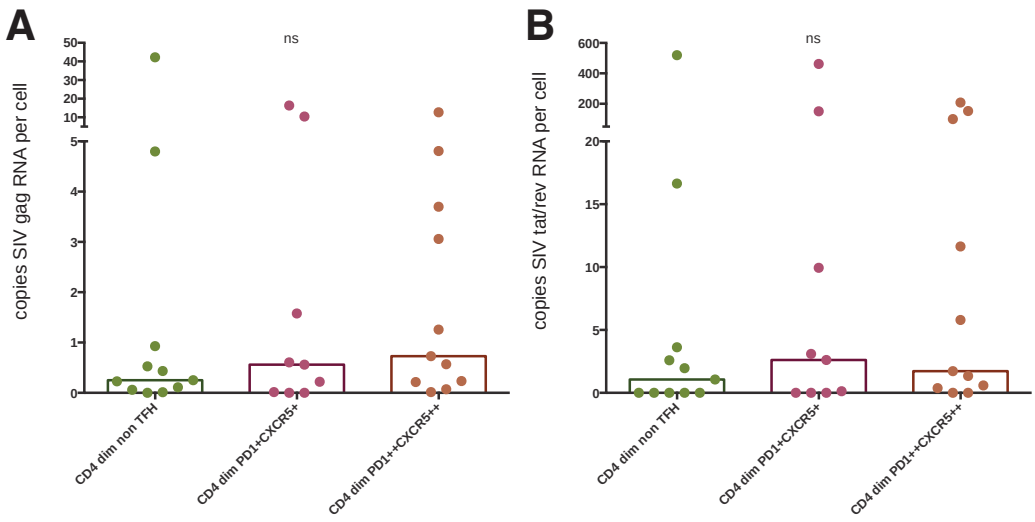

Fig 4.15 SIV RNA copies in CD4 dim T cell subsets. (A) unspliced gag RNA and (B) spliced tat/rev RNA copies per cell in non-TFH central memory, PD1+CXCR5+ central memory, and PD1++CXCR5++ central memory CD4 dim T cell subsets. No significant differences were found between population using one-way ANOVA.

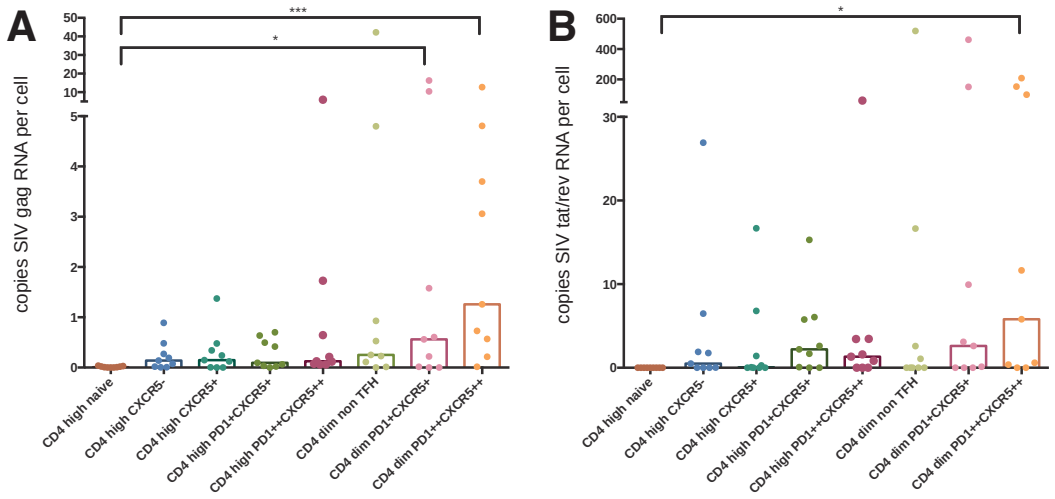

Fig 4.16 SIV RNA copies in CD4 bright and dim subsets. (A) unspliced gag RNA and (B) spliced tat/rev RNA copies per cell in CD4 bright (naïve, central memory CXCR5-, CXCR5+PD1-, CXCR5+PD1+, and CXCR5++PD1++) and CD4 dim (non TFH, CXCR5+PD1+, and CXCR5++PD1++) cells. Significant differences were determined using a one way ANOVA test.

4.2.4 Quantifying SIV in CD4 T cell subsets throughout infection

4.2.4.1 Measuring spliced and unspliced RNA in subsets

To track the proportion of infection in lymph node memory T cells, we used serial lymph node biopsies from SIVmac251 infected macaques and quantified SIV DNA and spliced and unspliced RNA at 13, 28, 76, and 176 days post infection. Gag DNA copies were highest per cell at 13 and 28 days post infection in all T cell populations, and were significantly lower by 76 days and 176 days post infection (Fig 4.17). CXCR5++PD1++ cells had the highest DNA copy numbers per cell at all time points, from a mean of 0.49 copies/cell at 13 days post infection and declining to 0.21 copies/cell at 28 days and 0.073 copies /cell at 176 days. DNA copy numbers were similar in CXCR5+PD1+, CXCR5+PD1-, and CXCR5- populations at 13 and 28 days post infection, ranging from 0.070 to 0.19 copies/cell. In chronic infection, SIV DNA copies per cell were relatively unchanged between CXCR5+PD1+, CXCR5+PD1-, and CXCR5- populations, with 0.042 copies/cell, 0.025 copies/cell, and 0.037 copies/cell respectively. Overall, CXCR5++PD1++ are infected at a higher frequency (as measured by copies of SIV DNA per cell) in early infection, and this difference is consistent throughout infection. While SIV DNA shows a history of infection, it does not indicate whether a cell is productively infected and whether the proviral genome is replication competent. Thus, we measured SIV RNA to better gauge where infection and replication were occurring throughout infection.

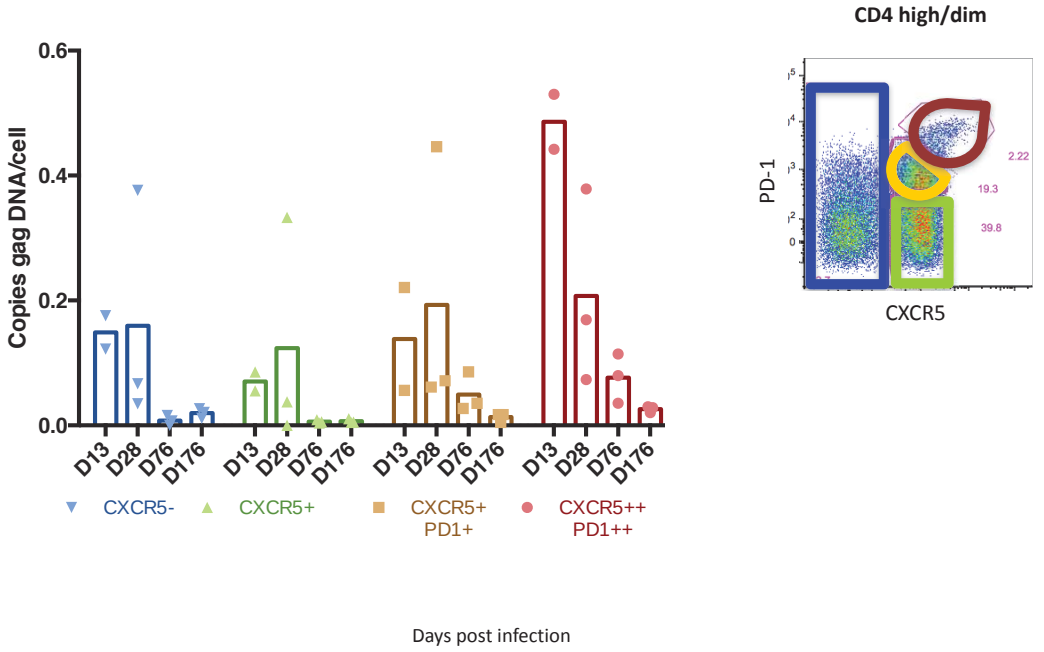

Fig 4.17 SIV gag DNA copies in CD4 bright and T cell subsets throughout infection. Copies of SIV gag DNA per cell at 13, 28, 76, and 176 days post infection in lymph node biopsies of SIV-infected macaques.

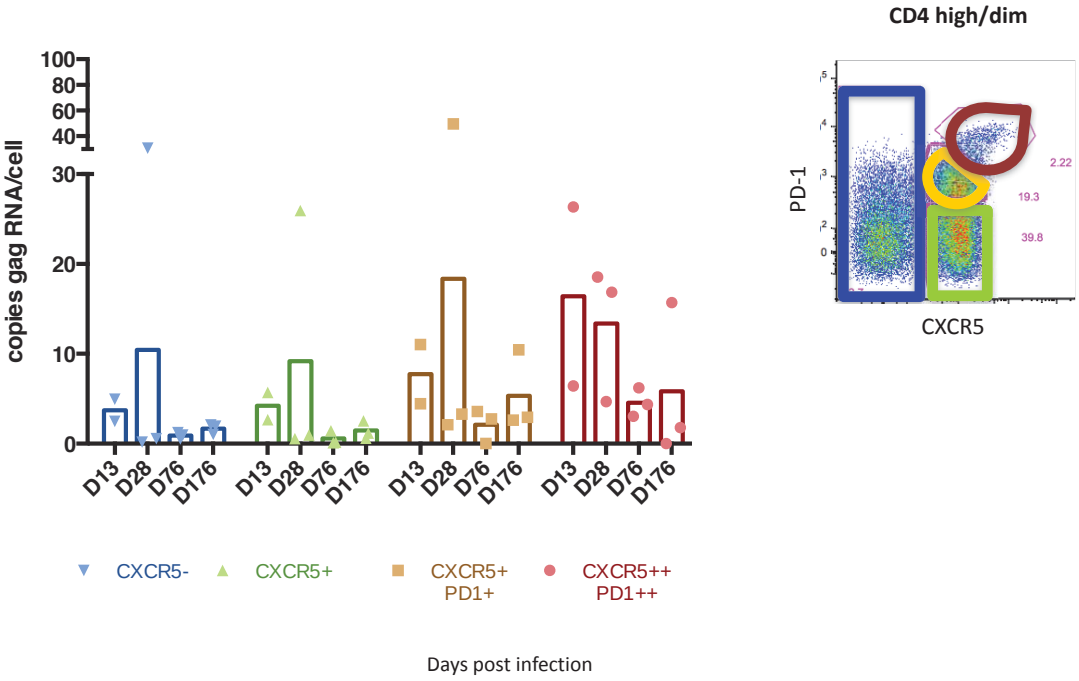

Fig 4.18 SIV unspliced gag RNA copies in CD4 bright and T cell subsets throughout infection. Left, copies of SIV gag RNA per cell at 13, 28, 76, and 176 days post infection in lymph node biopsies of SIV-infected macaques. Right, gating schematic for subsets of central memory CD4 T cells.

Gag RNA copies per cell had similar trends to DNA, with all T cell subsets from early time points (13 and 28 days) having higher copies per cell of unspliced RNA than later time points (means of 18 copies/cell to 3.7 copies/cell in acute samples vs. means of 5.8 copies/cell to 0.56 copies/cell in chronic) (Fig 4.18). CXCR5++PD1++ cells had the highest copy numbers of unspliced RNA per cell at 13 days, 76 days, and 176 days (16 copies/cell, 4.5 copies/cell, and 5.8 copies/cell), while CXCR5+PD1+ cells had the highest copies of gag RNA at 28 days

(18 copies/cell). CXCR5+PD1- cells and CXCR5- cells had lower copy numbers of gag RNA than CXCR5++PD1++ and CXCR5+PD1+ at all time points, but the difference was most dramatic at 76 days and 176 days, when they had on average fourfold fewer copies of SIV RNA per cell. Spliced Tat/rev RNA (Fig 4.19) had different dynamics, with variable copy numbers per cell across populations and over time. CXCR5++PD1++ cells and CXCR5+PD1+ cells had the highest copy numbers per cell of spliced RNA and were consistently above CXCR5- and CXCR5+PD1- cells. However, the net highest copy numbers per cell were measured at 76 days post infection in CXCR5++PD1++ cells. Due to the small numbers of cells sorted from each population (hundreds to thousands) and the low frequency of tat/rev producing cells in chronic infection, very low copy numbers per cell of tat/rev RNA were detected at 176 days post infection, and we were unable to measure tat/rev RNA in CXCR5++PD1++ cells. Overall, CXCR5++PD1++ cells and CXCR5+PD1+ cells contained higher copy numbers of spliced and unspliced RNA throughout infection, and the difference between RNA copy number per cell between these populations and CXCR5+PD1- and CXCR5- cells increased throughout infection.

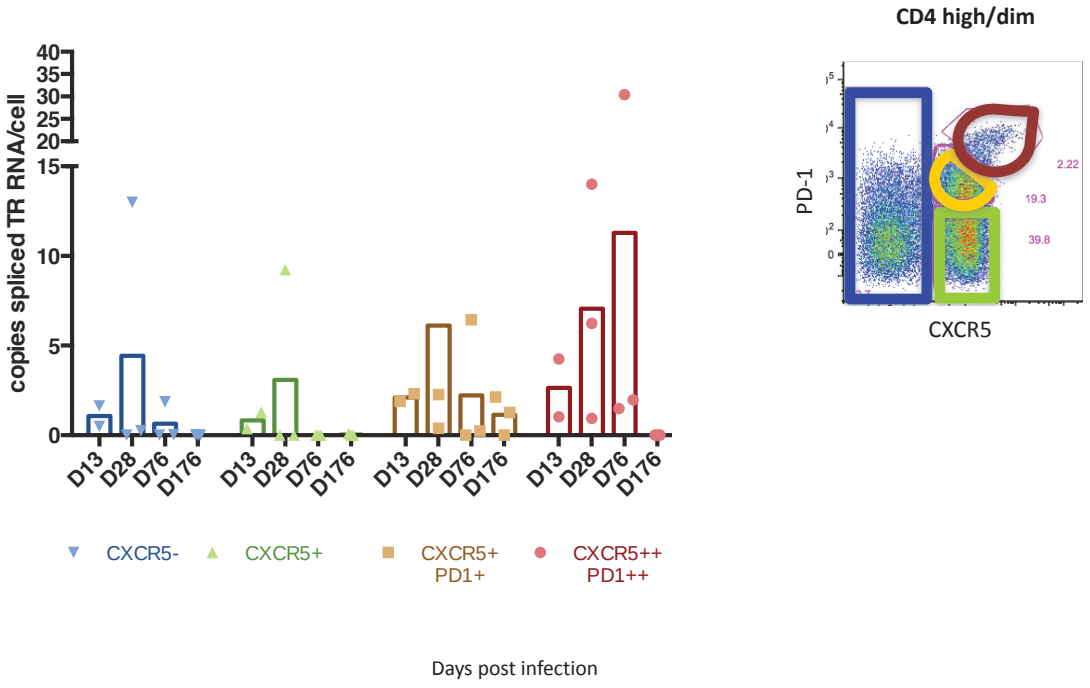

Fig 4.19 SIV spliced tat/rev RNA copies in CD4 bright and T cell subsets throughout infection. Left, copies of SIV tat/rev RNA per cell at 13, 28, 76, and 176 days post infection in lymph node biopsies of SIV-infected macaques. Right, gating schematic for subsets of central memory CD4 T cells.

Because of the low numbers of samples, we grouped acute (day 13/28) and chronic (day 76/176) samples to examine the compartmentalization of infection (Fig 4.20). In this analysis, gag DNA copies per cell was significantly higher in CXCR5++PD1++ cells than in CXCR5++ in both acute (mean of 0.32 copies/cell vs. 0.10 copies/cell) and chronic samples

(0.051 copies/cell vs. 0.0067 copies/cell). There was no statistical difference between gag RNA copies in subsets tin acute infection (although CXCR5++PD1++ and CXCR5+PD1+ cells had the highest copy number with means of 14.5 copies/cell and 14.1 copies/cell compared to 7.2 and 7.8 in CXCR5+PD1- and CXCR5-). In chronic infection, mean copies of gag RNA were significantly higher in CXCR5++PD1++ (3.2 copies/cell) than in CXCR5+PD1- (0.51 copies/cell) and CXCR5- (0.84 copies/cell), with CXCR5+PD1+ in between (1.5 copies/cell). Similarly in tat/rev RNA, there was no significant difference between copies per cell in acute infection (means of 2.2 copies/cell to 5.3 copies/cell), while in chronic infection CXCR5++PD1++ had the highest copy number of RNA per cell (mean of 7.9 copies/cell) and was significantly more than in CXCR5+ (0.18 copies/cell). Overall, productive infection was evenly distributed in acute infection (all subsets showed similar copy numbers of SIV RNA per cell), but in chronic infection, the bulk of infection was in CXCR5++PD1++ and CXCR5+PD1+ cells.

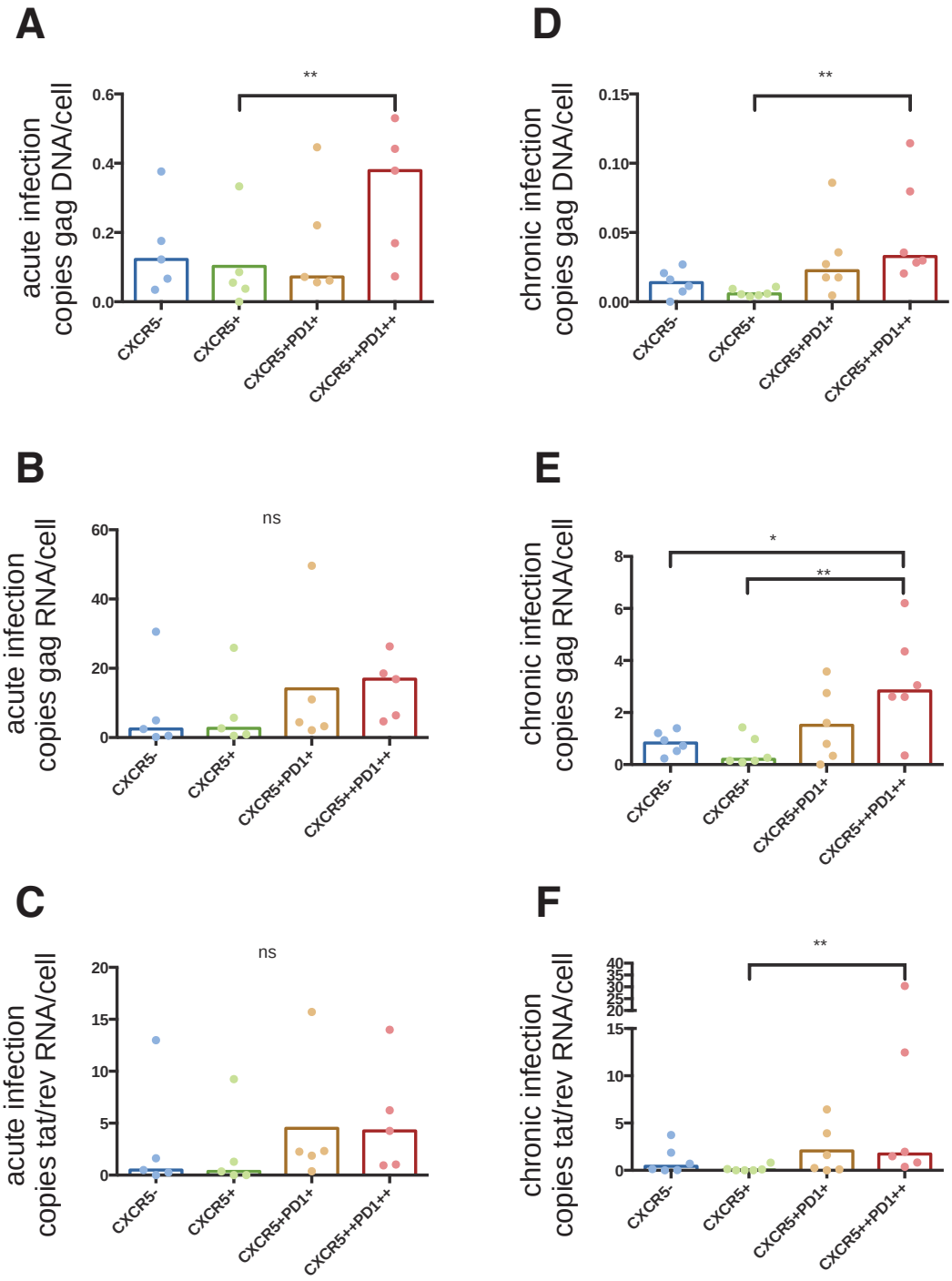

Fig 4.20 Distribution of SIV nucleic acids in acute and chronic infection. SIV RNA copies in CD4 bright and T cell subsets throughout infection. Copies of (A) gag DNA, (B) gag RNA and (C) tat/rev RNA in CXCR5- CXCR5+PD1-, CXCR5+PD1+, and CXCR5++PD1++ central memory CD4 T cells in acute infection. Copies of (D) gag DNA, (E) gag RNA and (F) tat/rev RNA in CXCR5- CXCR5+PD1-, CXCR5+PD1+, and CXCR5++PD1++ central memory CD4 T cells in chronic infection. Significant differences were determined using a one way ANOVA test.

4.2.4.2 Changes in TFH throughout infection

Previous studies have shown that TFH are increased as a fraction of all central memory T cell in lymph node in chronic HIV/SIV infection[170]. We confirmed this in our samples by

measuring the proportion of CXCR5++PD1++, CXCR5+PD1+, CXCR5+PD1-, and CXCR5- cells as a percentage of central memory (CD45RA-CCR7-CD28+CD95+) CD4 T cells (Fig. 4.21). CXCR5++PD1++ cells increased from a mean of 4.8% at 10/13 days post infection to 36% at 176 days post infection. CXCR5+PD1+ cells remained constant over the course of infection (18%-23% of central memory CD4 T cells). Both CXCR5+PD1- cells and CXCR5- cells decreased significantly over the course of infection, dropping from 19.4% to 2.8% and 51% to 32%, respectively. This shift in proportions of memory T cell subsets has an impact on the compartmentalization of virus replication and sites of infected cells.

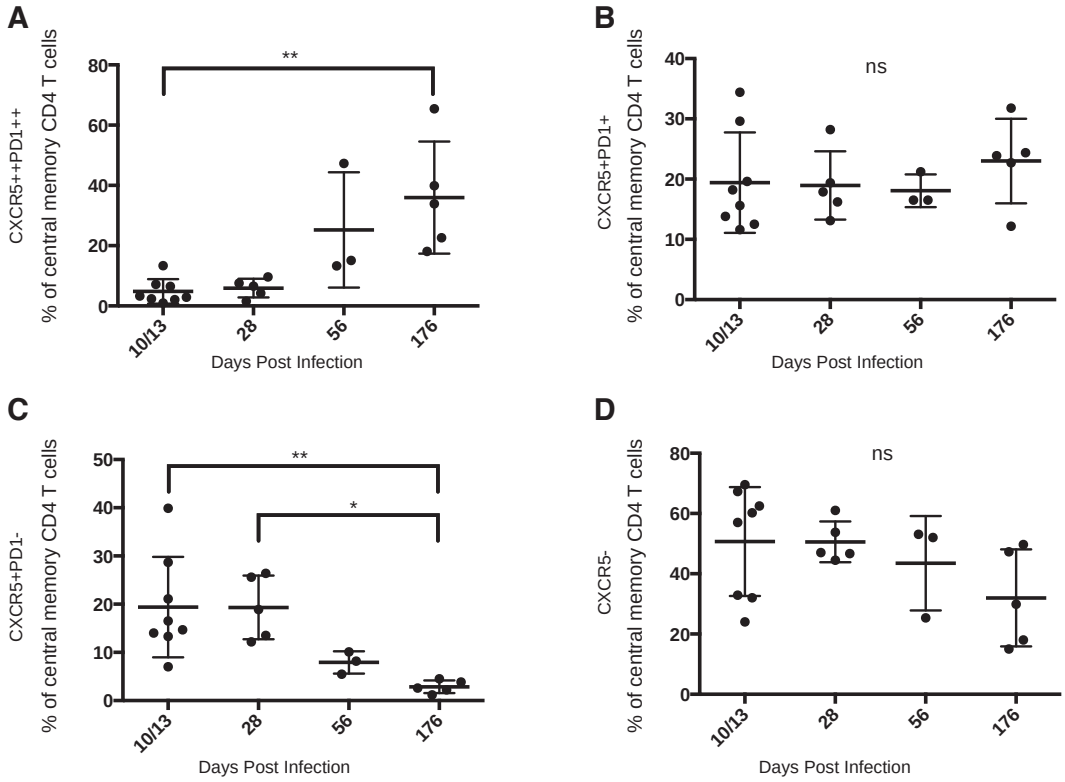

Fig 4.21 Frequencies of T cell subsets throughout infection. (A) CXCR5++PD1++, (B) CXCR5+PD1+, (C) CXCR5+PD1-, and (D) CXCR5- cells as a percentage of central memory CD4 T cells from early to late infection. Significant differences were determined using a one way ANOVA test.

While CXCR5++PD1++ and CXCR5+PD1+ cells had higher copy numbers of gag DNA and gag and tat/rev RNA per cell in all populations, the frequencies of CD4 T cell memory cells shift throughout the course of infection and impact the composition of the pool of infected cells. Using the viral nucleic acid copy numbers per cell and the proportion of each cell subset within the central memory, we can estimate the contribution of each subset to the total pool of SIV DNA and RNA (Fig. 4.22). In these calculations, we see that despite only representing a small percentage of all central memory T cells at peak infection, TFH (here defined as CXCR5++PD1++ and CXCR5+PD1+ cells) contain an outsized amount of gag DNA and gag and tat/rev RNA (40%, 49%, 46% respectively). At 28 days post infection when plasma

viremia had decreased to viral setpoint, these frequencies had diminished slightly (25%, 30%, and 29%), but later in infection, when TFH represent a higher fraction of all central memory cells, contribute most of viral DNA and RNA (73%, 84%, 99% at 176 days). In summary, CXCR5++PD1++ and CXCR5+PD1+ T follicular helper cells represent a significant source of SIV DNA and RNA in early infection, but by later infection are the major compartment of SIV infection and replication.

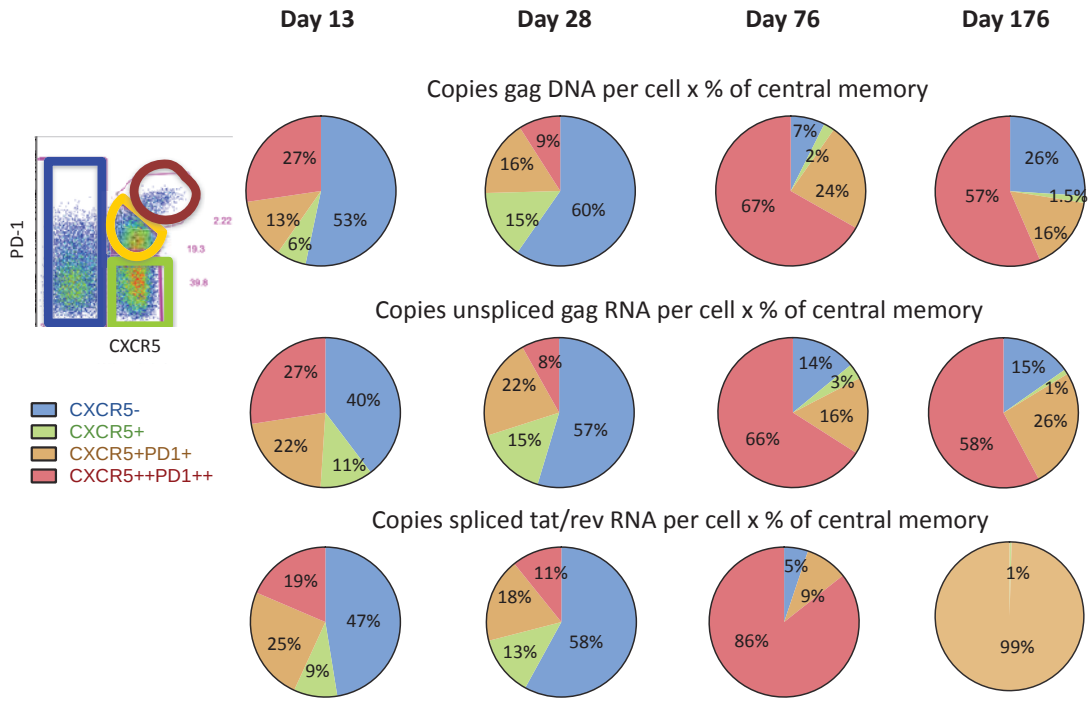

Fig 4.22 Contributions to SIV DNA and RNA from memory T cell subsets. Top, contributions to total gag DNA in central memory T cells by subset at 13, 28, 76, and 176 days post infection. Middle, contributions to total unspliced gag RNA in central memory T cells by subset at 13, 28, 76, and 176 days post infection. Bottom,, contributions to total spliced tat/rev RNA in central memory T cells by subset at 13, 28, 76, and 176 days post infection. Copies per cell of SIV DNA and RNA in four memory subsets were multiplied by the proportion of that subset in the total memory compartment to derive the contribution of each subset to the total pool of SIV.

4.2.5 RNA flow cytometry – detecting and phenotyping individually infected cells

4.2.5.1 Testing RNA probe staining

Quantifying viral nucleic acids yields detailed information of infection of bulk subsets of CD4 T cells, but does not directly yield the proportion of infection of different populations. Furthermore, populations must be stained and fixed in advance of DNA/RNA quantification, preventing the subsequent analysis of the features of infected cells within sorted populations. To gain a more detailed understanding of the cellular markers of infected cells, we used RNA probes in flow cytometry to identify individually infected cells. The use of RNA probes in flow cytometry is based upon techniques of *in situ* hybridization in fixed tissues, and has recently been developed as a commercially available kit [377]. We first tested the PrimeFlow kit (eBiosciences) against probes and reagents developed by ACD for use in RNAScope [378]

staining on formalin-fixed, paraffin-embedded tissue slices to determine which assay was more sensitive. Both assays are based on similar technologies and use branching amplified to RNA target probes with fluorescent detectors. We performed a side-by-side comparison of the two sets of probes, amplifies, and detectors to determine which assay had greater sensitivity (Fig. 4.23). While both ACD and eBiosciences reagents detected RNA-positive CD4 T cells from splenocytes at 13 days post infection, the eBiosciences reagents had better staining on central memory T cells and subsets. In the eBiosciences staining, 2.47% of central memory T cells were RNA probe-positive compared to 1.39% in the ACD protocol. The separation on the eBiosciences samples was better than on the ACD samples, with a separation of nearly two logs in the Biosciences samples and just over one log in the ACD samples. Both samples had equivalent background staining on cell populations not infected with SIV (CD8 T cells and CD3- cells) and on uninfected controls.

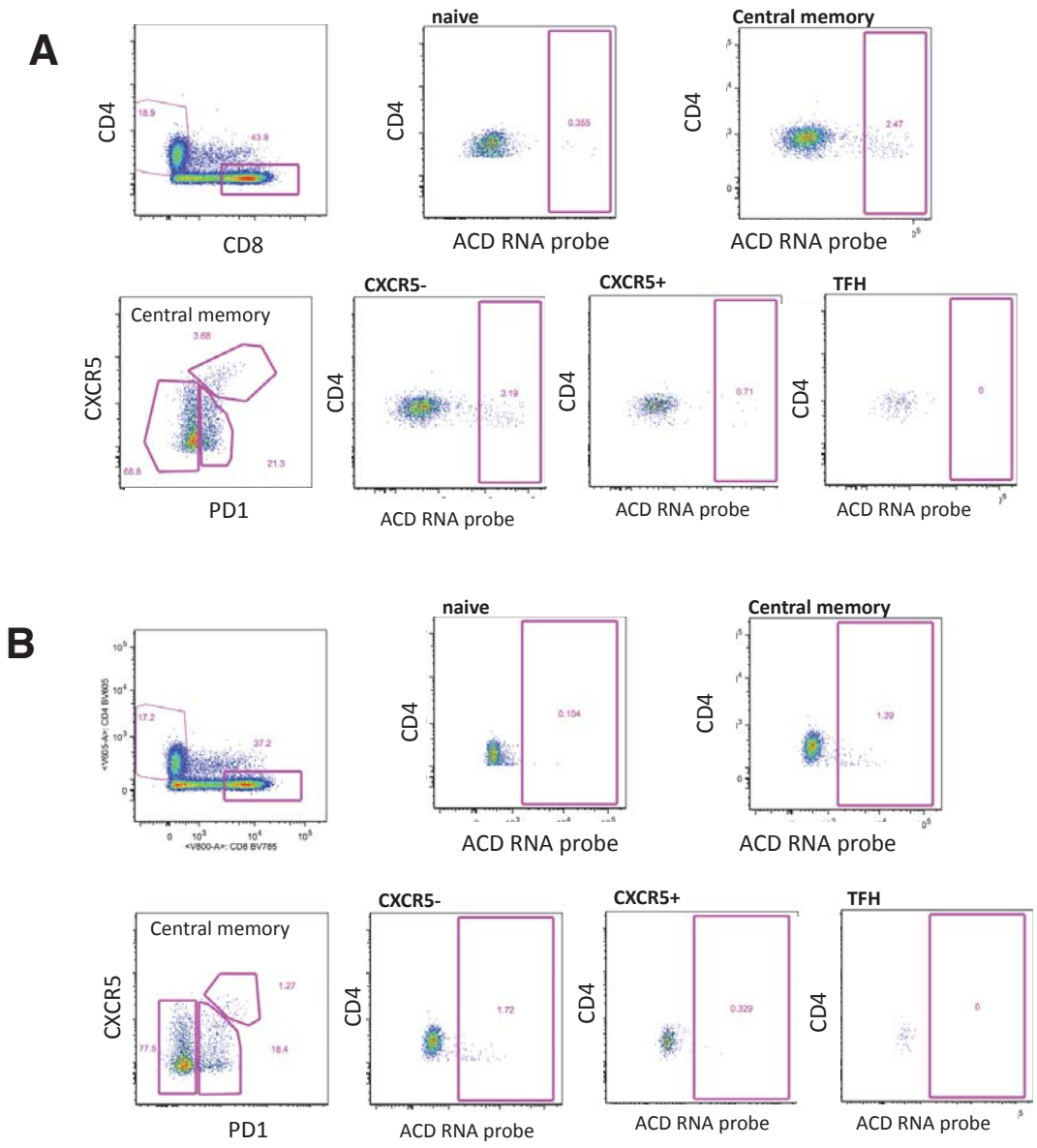

Fig. 4.23 Comparison of RNA flow cytometry staining using eBiosciences and ACD reagents. (A) eBiosciences regent staining and (B) ACD reagent staining of SIV infected splenocytes from 13 days post infection. In both figures, plots show staining of probe on naïve (top middle) and memory (top right) cells (from the CD4+CD8- compartment, top left), and from within the central memory compartment (CD95+CD28+), probe staining on CXCR5-, CXCR5+, and TFH (bottom row).

4.2.5.2 Specificity of RNAflow SIV probe staining

To confirm the specificity of the SIV RNA probes in infected cells, we used probes against beta-2 microglobulin (B2M) as a positive control and bacterial enzyme dapB as a negative control (Fig. 4.24). We observed no dapB staining on CD4 or CD8 cells, whereas 88-91% of CD4 and CD8 T cells were positive for B2M. Staining with SIV probes was specific to CD4 T cells (1.6% of CD4 T cells, isolated from splenocytes of an acutely infected macaque) and while there was background staining on CD8 T cells, it was significantly below staining on

CD4 cells. Nonetheless, we increased the number of wash steps in the protocol to reduce background staining.

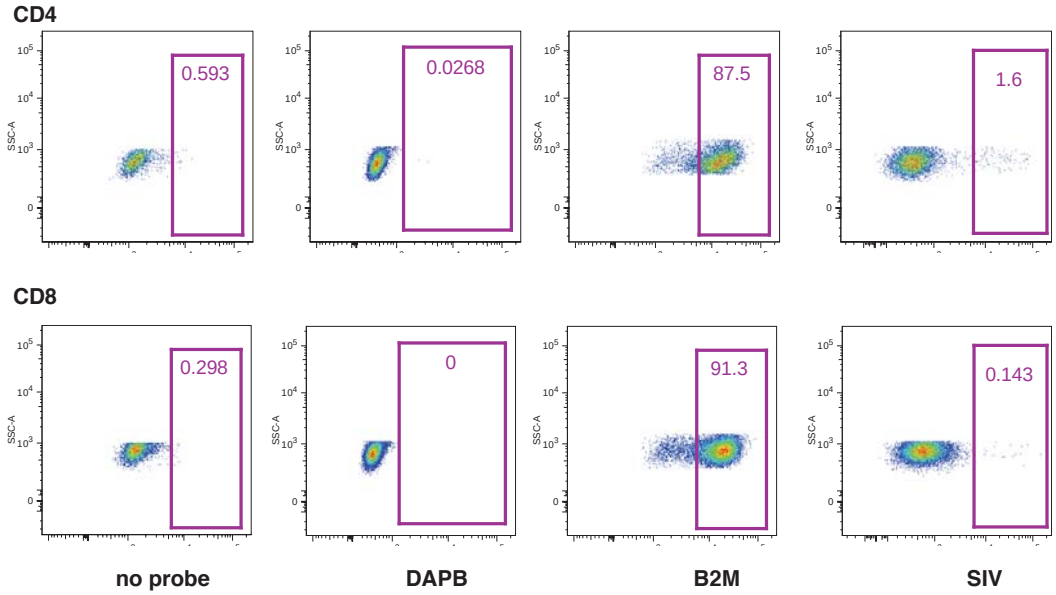

Fig 4.24 Staining of RNA flow probes and controls. Staining of DAPB (negative control), B2M (positive control), and SIV RNA probes alongside no probe control on (top row) CD4 T cells and (bottom row) CD8 T cells.

To further confirm the specificity of the RNA probes, we infected CEMx174 cells with SIVmac251 and measured the proportion of infected cells via intracellular p24 staining and RNA probe staining (Fig. 4.25). Samples at five days post infection showed clear p24 staining on CD4 down-regulated cells with an infection proportion of 8%, whereas staining at six days post infection with RNA probes had an infection frequency of 37.7%. The infection proportion is higher in RNA probe staining than with p24, as p24 is produced only at certain stages in the SIV lifecycle whereas SIV RNAs are present during initial infection and throughout the later stages of cellular infection, and the p24 probe is designed for HIV core antigen and shows only partial cross-reactivity with SIV proteins.

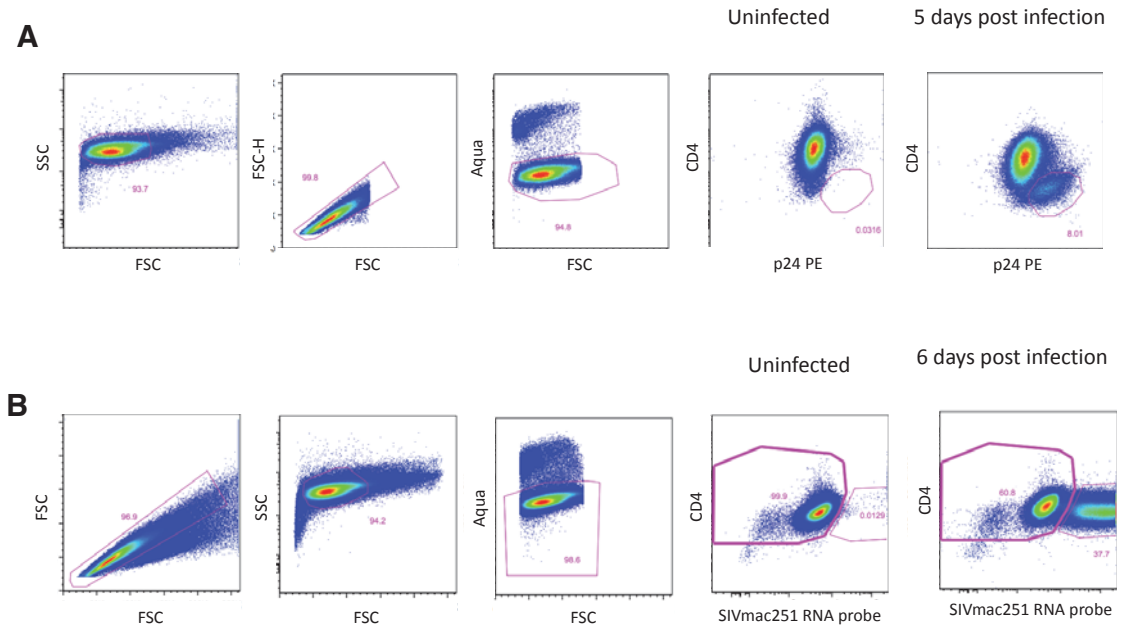

Fig 4.25 Infection and staining of cell lines with RNA flow probes. (A) Gating and staining of CEMx174 cells infected with SIVmac251 at zero and 5 days post infection. Cells were intracellularly stained with p24. (B) Gating and staining of CEMx174 cells infected with SIVmac251 at zero and six days post infection. Cells were stained with RNAflow SIV probes.

We developed a flow cytometry staining panel to evaluate the proportional infection of CD4 T cell subsets that was compatible with the long duration and high temperatures of the PrimeFlow protocol, which involves 18 wash steps, 6 hours of incubation at 40°C for 6 hours, and fourteen hours from the start of the protocol to acquisition of samples (Fig. 4.26). In addition, not all commercially available fluorophores are compatible with the PrimeFlow buffers and reagents, so a minimal panel was designed to accommodate the limitations of the kit while still differentiating CD4 T cell memory subsets and TFH in particular. To confirm the gating and staining after the PrimeFlow protocol, for each sample we stained a subset of cells with the surface panel only and fixed and acquired the samples without undergoing the incubations and washes. While there were some differences in the fluorescence between the two protocols, we could confidently distinguish the cellular populations in the full protocol samples. In all infected samples, we also ran a no-probe control to account for nonspecific binding of the amplifiers and label probes. This fluorescence –minus-one control was used to set the gating for probe-positive samples in all infected samples.

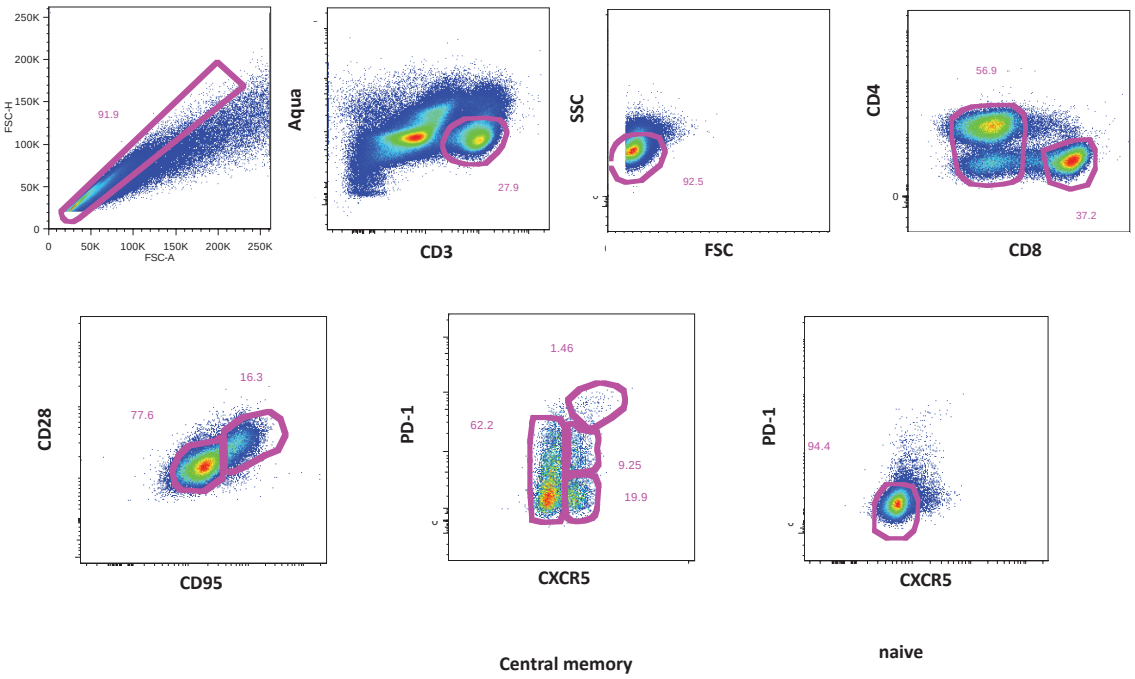

Fig 4.26 Representative gating schematic for RNA probe staining from SIV-infected lymph node biopsies. Lymph node single cell suspensions were stained and acquired on a flow cytometer after gating on forward/side scatter, lymphocytes, live -CD8- CD3+ T cells. Memory cells were defined as CD28+CD95+ and subsequently gated on expression of CXCR5 and PD-1. Gates were set based on staining on naïve and CD8 T cells. For all samples, a no-probe FMO control was stained alongside a surface-only sample to ensure accurate gating of cell populations

Probe staining on acutely infected and chronically infected lymph node samples showed that SIV probe staining is primary on CD4 T cells, with only minimal background on CD8 T cells (Fig. 4.26). When CD4 T cells were gated on CD28 and CD95 to differentiate naïve and central memory populations, the proportion of infection on central memory cells was over tenfold higher than in naïve cells. Acutely infected animals (5-13 days post infection) had significantly higher frequencies of infection than animals that had controlled viremia to viral setpoint (28/76 days post infection) or chronically infected animals (6 months-2 years post infection). Staining on uninfected animals showed only minimal background staining on CD4 and CD8 T cells and on central memory and naïve CD4 T cells, comparable to staining on CD8 T cells in infected animals. Acutely infected animals have a higher proportion of SIV-infected cells, and we wanted to confirm that we could distinguish chronically infected cells from background staining of RNA probes. Background staining in acutely and chronically infected samples varied from sample to sample (Fig. 4.27), but was reliably below the probe-positive samples at 176 days and 2 years post infection. Thus the RNA probes are specific to productive infection in CD4 T cells, and follows expected distributions of infection based on cellular phenotype.

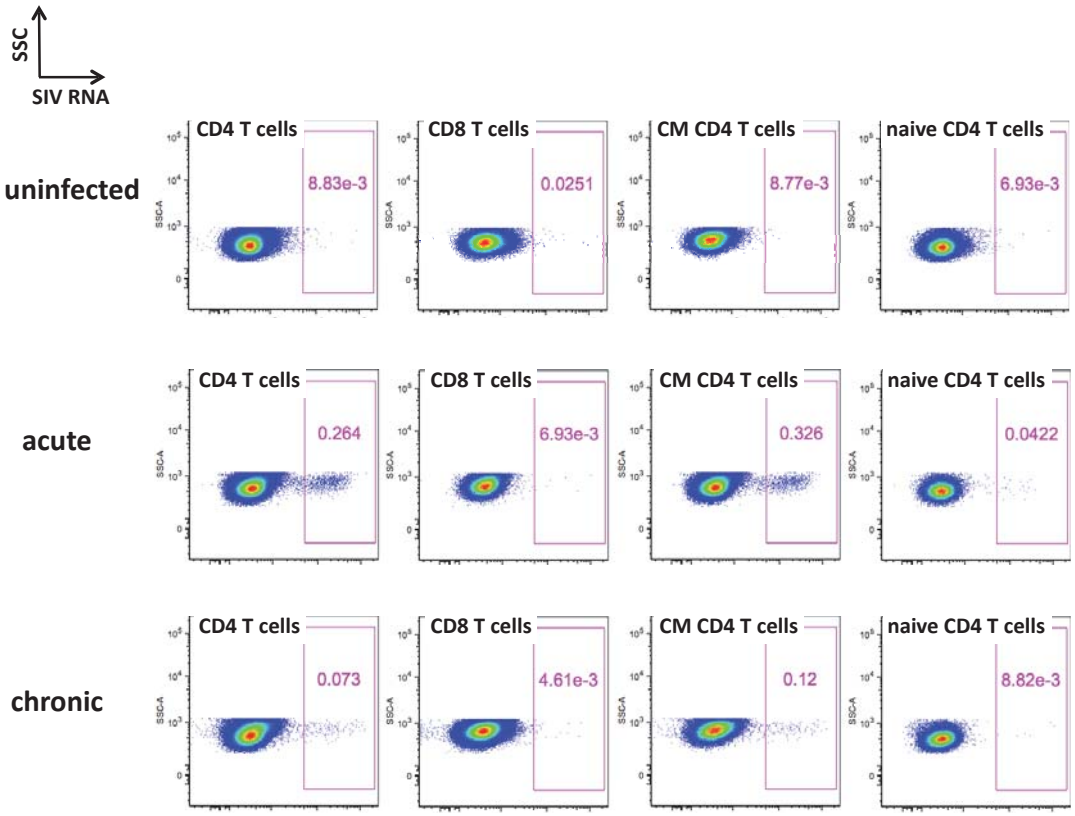

Fig 4.27 Staining of RNA flow probes on CD3 T cell populations. Staining of SIV probes on uninfected (top), acutely infected (middle), and chronically infected (bottom) lymph nodes CD4 T cells (far left column), CD8 T cells (left), central memory CD4 T cells (right), and naïve CD4 T cells (far right).

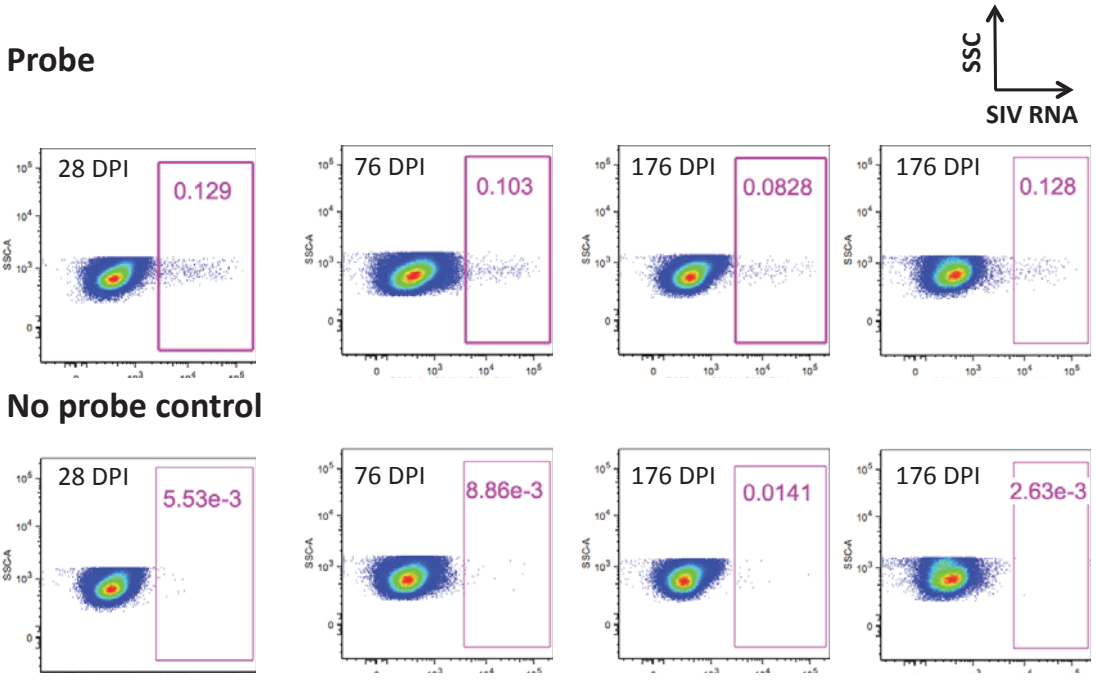

Fig 4.28 RNA probe staining on chronically infected lymph nodes. To test the background staining of the amplifiers used to detect the RNA probes, CD4 T cells from SIV-infected samples from 28 days (far left), 76 days (left), and 176 days (right and far right, two separate specimens) were stained with SIV RNA probes (top row) and compared to FMO controls (bottom row).

4.2.5.3 Staining is specific to memory T cell populations

We used CXCR5 and PD-1 to distinguish TFH in the RNA flow samples, and measured the proportion of RNA probe positive cells within four central memory populations. The highest proportions of infection were at 7-13 days post infection, when plasma virus levels were at or near peak. CXCR5++PD1++ cells had the highest proportion of infection (mean 1.5%), followed by CXCR5+PD1+ and CXCR5- (0.9% and 0.8%) and CXCR5+PD1- cells have the lowest proportion of infection (0.5%). By 1-3 months post infection when plasma virus was at setpoint, the proportion of RNA positive cells had declined significantly in CXCR5-, CXCR5+PD1-, and CXCR5+PD1+ cells to 0.32% to 0.56%. However, CXCR5++PD1++ cells still had a significantly higher proportion of infection at 1.67%. In chronic infection, the proportion of RNA probe positive cells declined in CXCR5-, CXCR5+PD1-, and CXCR5+PD1+ cells (ranging from 0.18% to 0.06%) but remained highest in CXCR5++PD1++ at 0.32%. Thus, TFH as defined by CXCR5 and PD1 staining are consistently infected at higher rates than other memory T cells, but this difference is most pronounced in later infection.

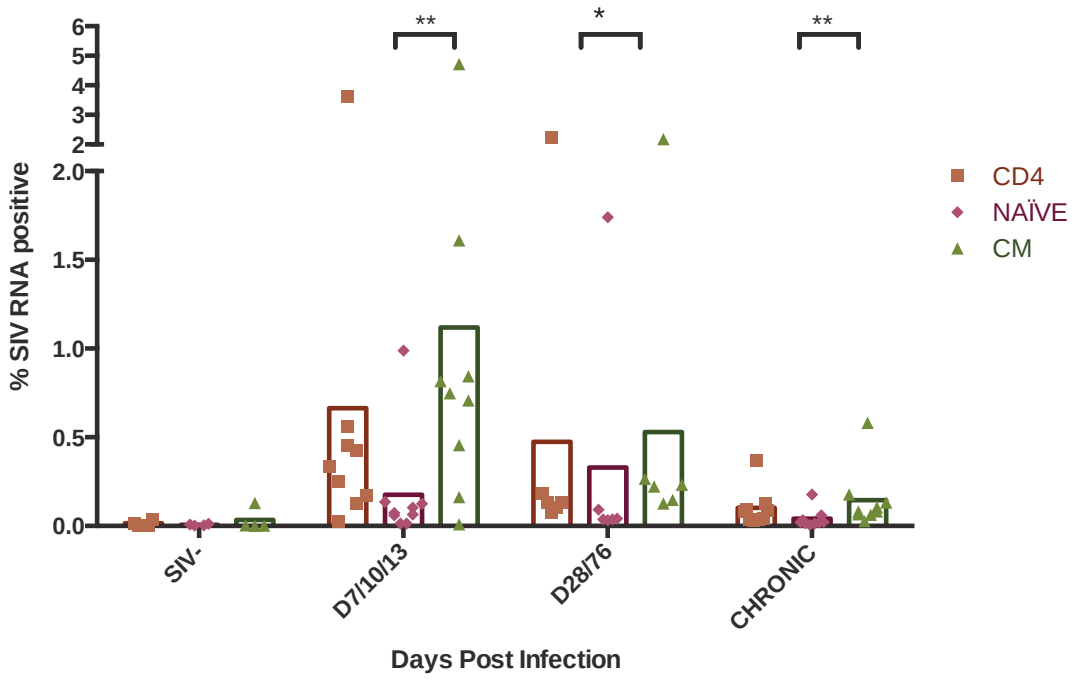

Fig 4.29 Frequencies of RNA probe staining on CD4 T cells. Percentage of RNA probe-positive cells in uninfected, 7/10/13 days post infection, 28/76 days post infection, and chronically infected lymph node biopsies. Within CD4 cells, samples were divided into naïve and central memory (CM) cells based on expression of CD95 and CD28. Significant differences were determined using a one way ANOVA test.

4.2.5.4 Results on acute samples, chronic

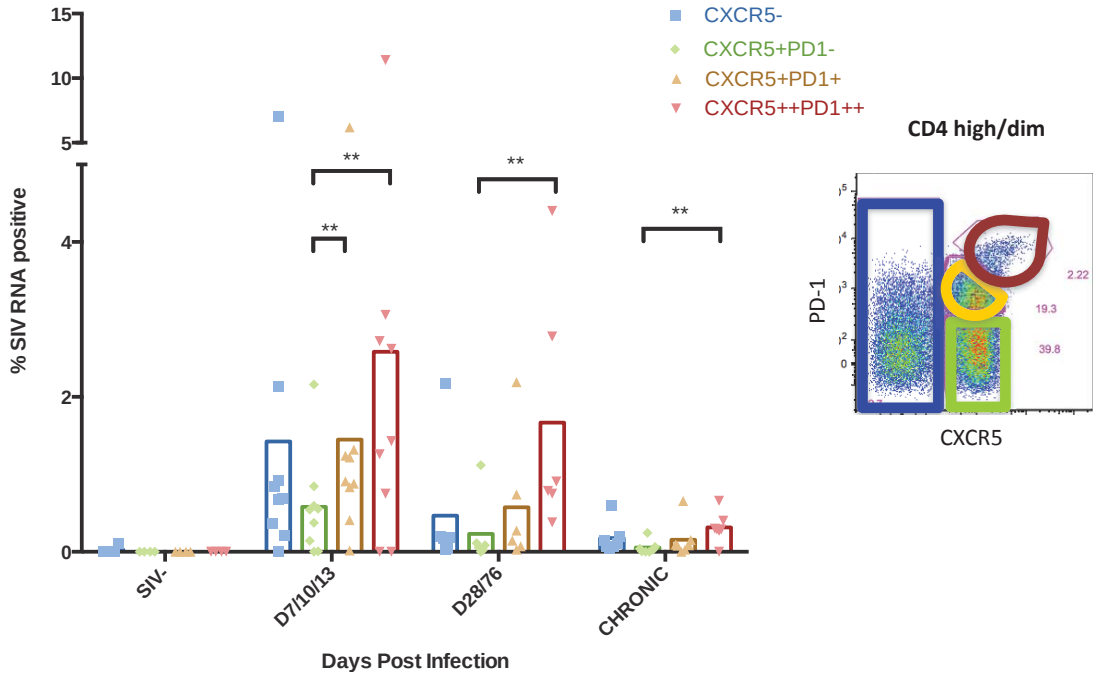

Fig 4.30 Frequencies of RNA probe staining on memory T cell subsets. Percentage of RNA probe-positive cells in CXCR5/PD1 subsets in uninfected, 7/10/13 days post infection, 28/76 days post infection, and chronically infected lymph node biopsies. Significant differences were determined using a one way ANOVA test.

While the increased proportion of SIV RNA-positive TFH compared to other T cells is significant on its own, when examined in the context of the relative frequencies of the central memory T cell populations is more notable. As described earlier in this thesis and in previously published work, the proportion of TFH as a proportion of memory T cells increases in chronic infection, with TFH representing up to 50% or more of central memory T cells in chronic infection. By multiplying the proportion of RNA probe positive cells in each population by that population's proportion in the total central memory pool, we can measure the contribution of each population to the total pool of virus-producing cells (Fig. 4.30). In acute samples, when TFH make up only a small percentage of memory T cells, in spite of having a higher proportion of infection only make a small contribution to infected cells (3% from CXCR5++PD1++ and 9% from CXCR5+PD1+). However, by 28 days post infection when plasma viremia had declined to viral setpoint and infection is largely under control, TFH contribute over 1/3 of all RNA probe positive cells (30% from CXCR5++PD1++ and 8% from CXCR5+PD1+). This trend continues into chronic infection, where TFH are responsible for nearly half of all RNA positive cells (37% from CXCR5++PD1++ and 11% from CXCR5+PD1+). This also shows that TFH are the major compartment of SIV replication and infection in chronic infection. This mirrors the qPCR/qRT-PCR data of SIV DNA/RNA copies per cell, indicating that T follicular helper cells contain the bulk of SIV

infection both in absolute quantities of viral nucleic acids and in proportion of SIV infected cells.

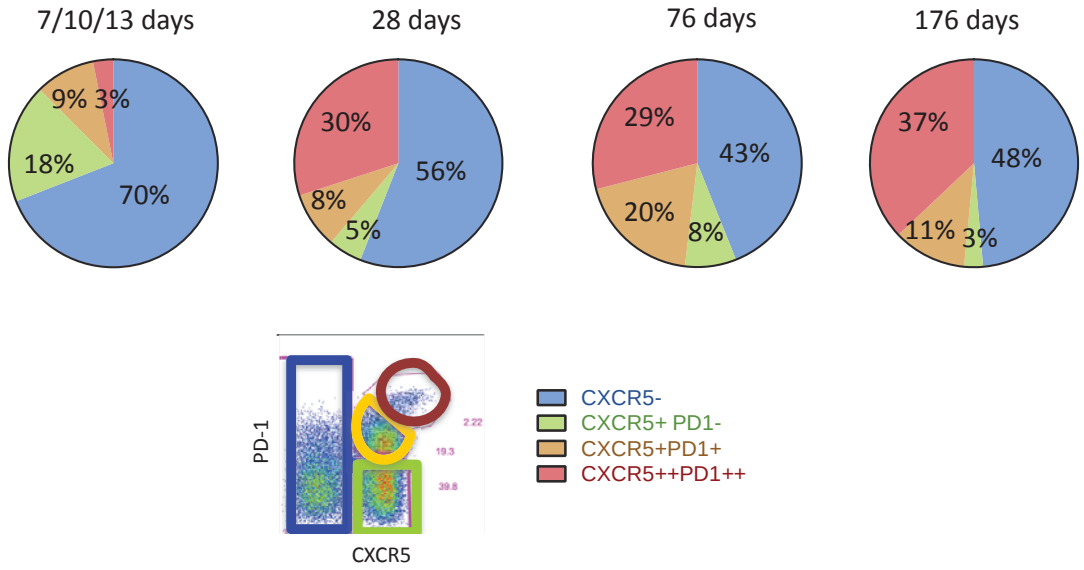

Fig 4.31 Contributions to SIV infected cells from subsets of central memory CD4 T cells. Percentage of RNA probe-positive cells multiplied by the fraction of the central memory yields the net contribution of CXCR5-, CXCR5+PD1-, CXCR5+PD1+ and CXCR5++PD1++ cells to the total pool of infected cells.

4.3 Conclusions

HIV/SIV rapidly infects and depletes CD4 T cells from the periphery and secondary lymphoid organs before being brought under partial control by the host immune system[36]. Even in the absence of clinical symptoms during the latent phase of infection, viral replication is on-going in lymph nodes and induces major changes in the phenotype and function of CD4 T cells [379,380]. While HIV/SIV infection requires at minimum expression of CD4 and a co-receptor (CCR5 or CXCR4), only a fraction of "eligible" CD4 T cells are infected[381]. A detailed understanding of the precise features and markers of the infected cells that harbour replication-competent virus is critical to the design of therapeutic antibodies (such as bispecific antibodies that can direct killing of infected cells) and cure strategies (demarcating the latent reservoir). We observed several changes in the expression of cell surface markers on CD4 T cells in lymph nodes during acute and chronic infection, reflecting increased immune activation and perturbations in T cell subsets. Acutely infected samples had high CD127 expression and low ICOS expression, whereas chronically infected samples had higher ICOS expression and higher SLAM expression than uninfected samples. TFH had distinct patterns of chemokine and activation marker expression when compared to CXCR5- and CXCR5+ CD4 T cells, with lower CCR4, ICOS, and CD25.

TFH are particularly important in HIV/SIV infection because of their role in providing B cell help to generate an effective antibody response. Accumulation of TFH, and their preferential infection in chronic infection, has been reported [170,172], and we examined the history of infection of TFH from early to chronic infection. We designed primers and probes to detect spliced SIV RNAs, to differentiate between cells that were infected by SIV and had an integrated proviral genome (and would therefore show infection via DNA qPCR), and cells that bypassed any cellular restriction and were capable of transcribing viral genes (as evidenced by the presence of spliced and unspliced RNA). Early in infection, most subsets of T cells were equally infected by DNA and RNA qPCR, likely reflecting the availability of target cells and the lack of an effective host immune response. In later infection, follicular T cells had higher copy numbers of both SIV DNA and RNA per cell. This indicates TFH are not only more infected (containing a proviral genome) than other populations, but also produce more viruses (indicated by transcription of viral RNAs) in chronic infection.

Assaying the proportion of infected cells by measuring nucleic acids from bulk sorted samples via FACS is limited in that populations of interest must be determined in advance of quantifying nucleic acids. Information on the number of individual cells infected is lost in the bulk extraction of DNA and RNA, and even clearly delineated subsets of T cells show variable expression of surface markers. We used novel SIV RNA probes in a flow cytometry assay to measure individually infected cells within lymph node populations, allowing us to calculate the proportion of infection within TFH and non-TFH throughout infection. We found that in acute infection, follicular T cells make up only a small percentage of SIV RNA producing cells, but by chronic infection contain the bulk of viral RNAs. The role of follicular T cells as the major compartment of SIV infection and replication is intensified by the relative increase in the proportion of TFH (as a fraction of central memory T cells) from acute to chronic infection. CXCR5+PD1+ and CXCR5++PD1++ CD4+ T cells are not only infected at a higher frequency than other T cells, but make up a greater fraction of the lymph node CD4+ T cells in chronic infection.